



HAL
open science

Young Sprague Dawley rats infected by *Plasmodium berghei*: A relevant experimental model to study cerebral malaria

Sokhna Keita Alassane, Marie-Laure Nicolau-Travers, Sandie Ménard, Olivier Andreoletti, Jean-Pierre Cambus, Noémie Gaudre, Myriam Włodarczyk, Nicolas Blanchard, Antoine Berry, Sarah Abbes, et al.

► To cite this version:

Sokhna Keita Alassane, Marie-Laure Nicolau-Travers, Sandie Ménard, Olivier Andreoletti, Jean-Pierre Cambus, et al.. Young Sprague Dawley rats infected by *Plasmodium berghei*: A relevant experimental model to study cerebral malaria. PLoS ONE, 2017, 12 (7), pp.e0181300. 10.1371/journal.pone.0181300 . hal-01595014

HAL Id: hal-01595014

<https://hal.science/hal-01595014>

Submitted on 26 Sep 2017

HAL is a multi-disciplinary open access archive for the deposit and dissemination of scientific research documents, whether they are published or not. The documents may come from teaching and research institutions in France or abroad, or from public or private research centers.

L'archive ouverte pluridisciplinaire **HAL**, est destinée au dépôt et à la diffusion de documents scientifiques de niveau recherche, publiés ou non, émanant des établissements d'enseignement et de recherche français ou étrangers, des laboratoires publics ou privés.



Distributed under a Creative Commons Attribution 4.0 International License

RESEARCH ARTICLE

Young Sprague Dawley rats infected by *Plasmodium berghei*: A relevant experimental model to study cerebral malaria

Sokhna Keita Alassane^{1,2,3}, Marie-Laure Nicolau-Travers^{1,2}, Sandie Menard⁴, Olivier Andreoletti⁵, Jean-Pierre Cambus⁶, Noémie Gaudre⁴, Myriam Wlodarczyk⁴, Nicolas Blanchard⁴, Antoine Berry⁷, Sarah Abbes^{1,2}, David Colongo⁸, Babacar Faye³, Jean-Michel Augereau^{1,2}, Caroline Lacroux⁵, Xavier Iriart^{4,7}, Françoise Benoit-Vical^{1,2}*

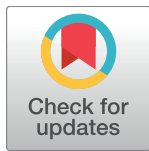
1 CNRS, LCC (Laboratoire de Chimie de Coordination), 205 route de Narbonne, Toulouse, France, **2** Université de Toulouse, UPS, INPT, Toulouse, France, **3** UFR Sciences de la Santé, Université Gaston Berger, St Louis, Sénégal, **4** CPTP (Centre de Physiopathologie de Toulouse Purpan), INSERM U1043, CNRS UMR5282, Université de Toulouse III, Toulouse, France, **5** UMR INRA ENVT 1225, Interactions Hôte Agent Pathogène, Ecole Nationale Vétérinaire de Toulouse, 23 Chemin des Capelles, Toulouse, France, **6** Laboratoire Hématologie, Centre Hospitalier Universitaire, Toulouse, France, **7** Service de Parasitologie-Mycologie, Centre Hospitalier Universitaire, Toulouse, France, **8** Hyphen-stat, 195 route d'Espagne, Toulouse, France

☞ These authors contributed equally to this work.

✉ Current address: Service de Pneumologie, Institut du thorax, Centre Hospitalier Universitaire, Nantes, France

‡ These authors also contributed equally to this work.

* Francoise.Vical@inserm.fr



OPEN ACCESS

Citation: Keita Alassane S, Nicolau-Travers M-L, Menard S, Andreoletti O, Cambus J-P, Gaudre N, et al. (2017) Young Sprague Dawley rats infected by *Plasmodium berghei*: A relevant experimental model to study cerebral malaria. PLoS ONE 12(7): e0181300. <https://doi.org/10.1371/journal.pone.0181300>

Editor: Leonardo Jose de Moura Carvalho, Instituto Oswaldo Cruz, BRAZIL

Received: September 28, 2016

Accepted: June 14, 2017

Published: July 24, 2017

Copyright: ©2017 Keita Alassane et al. This is an open access article distributed under the terms of the [Creative Commons Attribution License](https://creativecommons.org/licenses/by/4.0/), which permits unrestricted use, distribution, and reproduction in any medium, provided the original author and source are credited.

Data Availability Statement: All relevant data are within the paper and its Supporting Information files.

Funding: The authors thank the French Centre National de la Recherche Scientifique (CNRS) for financial support and the Senegalese “Ministère de l’Enseignement Supérieur et de la Recherche” for the Ph.D. grant of SKA. The funders had no role in study design, data collection and analysis, decision to publish, or preparation of the manuscript.

Abstract

Cerebral malaria (CM) is the most severe manifestation of human malaria yet is still poorly understood. Mouse models have been developed to address the subject. However, their relevance to mimic human pathogenesis is largely debated. Here we study an alternative cerebral malaria model with an experimental *Plasmodium berghei* Keyberg 173 (K173) infection in Sprague Dawley rats. As in Human, not all infected subjects showed cerebral malaria, with 45% of the rats exhibiting Experimental Cerebral Malaria (ECM) symptoms while the majority (55%) of the remaining rats developed severe anemia and hyperparasitemia (NoECM). These results allow, within the same population, a comparison of the noxious effects of the infection between ECM and severe malaria without ECM. Among the ECM rats, 77.8% died between day 5 and day 12 post-infection, while the remaining rats were spontaneously cured of neurological signs within 24–48 hours. The clinical ECM signs observed were paresis quickly evolving to limb paralysis, global paralysis associated with respiratory distress, and coma. The red blood cell (RBC) count remained normal but a drastic decrease of platelet count and an increase of white blood cell numbers were noted. ECM rats also showed a decrease of glucose and total CO₂ levels and an increase of creatinine levels compared to control rats or rats with no ECM. Assessment of the blood-brain barrier revealed loss of integrity, and interestingly histopathological analysis highlighted cytoadherence and sequestration of infected RBCs in brain vessels from ECM rats only. Overall, this ECM rat model showed numerous clinical and histopathological features similar to Human CM and appears to be a promising model to achieve further understanding the CM

Hyphen Stat provided only support in the form of salaries for author DC, but did not have any additional role in the study design, data collection and analysis, decision to publish, or preparation of the manuscript. The specific roles of these authors are articulated in the 'author contributions' section.

Competing interests: This does not alter our adherence to PLOS ONE policies on sharing data and materials.

pathophysiology in Humans and to evaluate the activity of specific antimalarial drugs in avoiding/limiting cerebral damages from malaria.

Introduction

Malaria remains a “major killer of children” in one of its more severe aspects, Cerebral Malaria (CM), with a fatality rate of 15–25% in African children despite effective antimalarial chemotherapy [1]. CM causes 78% of all malaria deaths. It is caused by the apicomplexan parasite *Plasmodium falciparum*, affecting not only children under the age of 5, but also pregnant women and non-immune patients such as tourists in endemic areas [2–4]. This pathology is an acute encephalopathy characterized by fever, vomiting, headache, seizure, respiratory distress, malarial retinopathy, impaired consciousness and/or coma [2,5–7].

Despite its well-documented clinical signs, the pathogenesis of Human CM is still unclear. Moreover, human CM is not a single pathological entity. Establishing correlations between clinical signs and cerebral lesions requires autopsies that are not easily accepted in countries where CM is endemic, and consequently only rarely performed [8]. Therefore, a reliable surrogate is crucial to get better insights into the pathophysiology of Human CM. In this framework, non-human primates would be the best model for malaria research [9], but their use is limited by financial, technical and ethical constraints. Rodent models are widely used permitting brains studies at different phases of the illness.

Thanks to the mouse experimental model of *Plasmodium berghei* infection, some particular points of CM pathogenesis, such as brain tissue inflammation, were highlighted [10]. However, given the considerable differences between the mouse and Humans, especially concerning the immune response, the relevance of the malaria mouse model is largely debated [9–16]. Indeed, the different mouse strains used in the laboratory gave highly variable experimental infection responses. Moreover, the ECM histopathological signs in mice are different from those of humans, and more specifically with regard to parasite sequestration, which is considered a crucial issue in Human CM occurrence [13,17,18]. Furthermore, experimental mouse models are frequently condemned as poor predictors for translational studies especially for the development of experimental drugs that may be ineffective in human pathologies [16]. Hence, it would be useful to establish an accessible and more relevant ECM model than mouse.

In parasitic diseases such as schistosomiasis, the rat model showed strong immunological similarities to Humans [19]. Moreover, the rat has been described as a relevant model for malaria [20–24] and for a lot of neurological studies [25–27]. In this context we assessed the relevance of the rat model in the study of ECM pathophysiology. We infected Sprague Dawley (SD) rats by the *P. berghei* K173 (here written later K173) strain and analyzed the different features of the model such as neurological signs, breakdown of the blood brain barrier (BBB), histological brain damage, immune response and hematological parameters in relation with the parasitemia and features reported in Human CM cases.

Results and discussion

Clinical features of ECM in SD rat

Infected SD rats were monitored to characterize the clinical outcome of ECM on K173 infection. Globally, K173 infection led to a severe form of malaria and a fatal outcome for 85% of the SD rats ($n = 34$). Infected SD rats presented either ECM with ascendant paraplegia, or severe anemia associated with malaria hyperparasitemia (namely NoECM *i.e.* without ECM

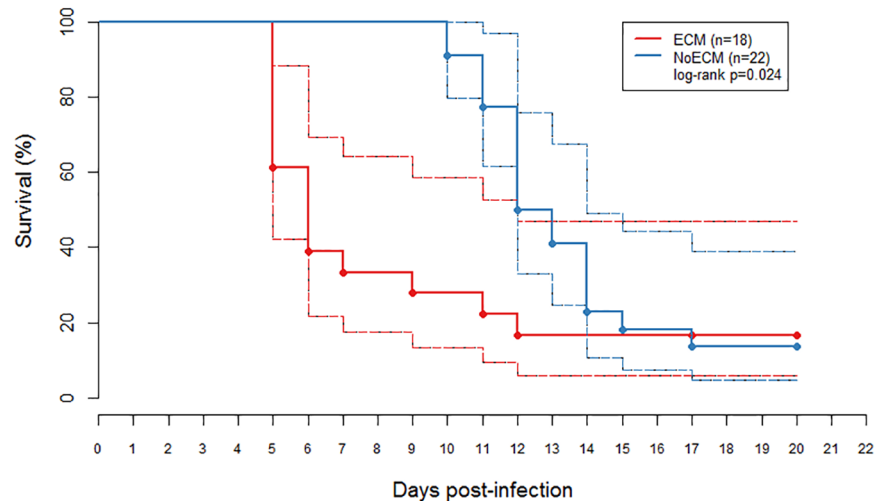


Fig 1. Kaplan-Meier curve estimate of a survival, with 95% confidence limits, of young Sprague Dawley (SD) rats with Experimental Cerebral Malaria (ECM; n = 18) and without Experimental Cerebral Malaria (NoECM; n = 22) after K173 infection. The solid lines are the survival curves and the dashed lines are the confidence intervals. Except for 6 rats (3 ECM and 3 NoECM), which cured spontaneously and were sacrificed at day 20, all the infected rats died at the latest on the 17th day *pi*. ECM rats died spontaneously between days 5 and 12 while the first cases of fatal outcomes for NoECM rats occurred on day 10. The difference between two groups was significant ($p = 0.024$).

<https://doi.org/10.1371/journal.pone.0181300.g001>

signs). Fig 1 presents the survival curves of both ECM and NoECM rats. 18 out of 40 infected SD rats (45%) exhibited ECM symptoms. ECM occurred within 5 to 9 days post infection—*pi* (median = 5.5 IQR [5; 7]) with death between day 5 and day 12 *pi* (median = 6 IQR [5; 6]). 14 among the 18 ECM rats (77.8%) showed paresis that quickly evolved to limb paralysis, and then, to global paralysis, respiratory distress, coma and death within 12 hours. The 4 remaining ECM rats spontaneously reversed their limb paralysis within 24–48 hours; one died later of hyperparasitemia and severe anemia (day 12) and the 3 others became cured with a total parasite clearance, at days 18–20 post-infection (*pi*) (S1C Fig).

The 22 other rats of the 40 infected had no clinical signs of ECM, but presented symptoms of severe malaria with discoloration of skin and eyes, strong anemia and weight loss. 19 out of 22 NoECM rats died between days 10 and 17 (median = 12, IQR [11.25; 14]) (Fig 1) and 3 remaining NoECM rats developed mild malaria and survived after total parasite clearance (S1C Fig).

Our results are close to those already reported in SD rats infected by *P. berghei* ANKA [28,29]. Cerebral complications including paralysis, convulsion and coma with death around day 5–8 *pi* were also observed with C57BL/6 and CBA/J mice infected by *P. berghei* ANKA [30,31].

These ECM manifestations in SD rats are close to the most common complications of falciparum malaria in children [2,32,33] largely observed in Africa [32–38] the continent with the most cases of this pathology in terms of morbidity and mortality. According to WHO criteria, Human CM corresponds to a severe malaria with coma [4]. However children presenting CM can develop focal neurological signs, decerebrated posturing due to raised intracranial pressure, impairment of consciousness, behavioral changes, and convulsions. Although most children with CM regain consciousness after specific treatment within 48 hours and seem to make a full neurological recovery, approximately 20% die and up to 10% have persistent neurological after-effects including lack of sensitivity, hemiplegia, and quadriplegia [2,39]. The convulsions were absent in rat ECM and even though they are frequently observed in children with CM, this symptom is rarely reported in Human CM in adults [40]. The SD rat model presented thus many clinical features common to Human CM.

Parasitemia evolution in ECM and NoECM rats

The parasitemia in both ECM and NoECM groups was microscopically determined from day 3 *pi* and increased gradually (S1A Fig). Parasitemia of ECM rats varied from 6.3% when the first symptoms occurred to a maximum of 23% for the latest case recorded while parasitemia of NoECM rats could reach very high values (89%) leading to fatal severe anemia. One out of 4 ECM rats which spontaneously reversed their limb paralysis, died later with hyperparasitemia (47%) while the 3 other ECM rats, showed total parasite clearance at days 18–20 *pi* after the parasitemia reached $38 \pm 4.5\%$ at day 12 *pi* (S1C Fig). Three NoECM rats developed mild malaria and showed a total parasite clearance at days 16–20 *pi* after a parasitemia peak of $26.3 \pm 2.1\%$ at day 12 *pi* (S1C Fig).

The difference in the course of the parasitemia between the two groups (ECM vs NoECM) was not statistically significant over a comparable period (Fig 2A). Fatal ECM events always occurred at a parasitemia inferior or equal to 23%. By contrast no NoECM rats died under a 30% parasitemia (Fig 2B) allowing the statistical threshold of 27.5% separating both groups. However neither the levels of parasitemia nor its kinetics are discriminant criteria for the prediction of ECM appearance in the rat model.

We can hypothesize that ECM outcome is not only dependent on the parasite virulence but also on the host SD rats. These animals are non-consanguine and each individual displays its intrinsic physiological sensitivity to the parasite. However, this SD rat model has the advantage of allowing a comparison within the same population of rats of the effects of the infection between ECM and severe malaria no ECM through the follow-up of biological, clinical and histological parameters. Even though parasitemia associated with Human CM is undocumented, according to WHO criteria, a high density of parasites in the blood (> 4%) increases the risk of deterioration to severe malaria [4]. However low parasitemia are linked with human CM occurrence [41].

ECM in SD rat is not associated to anemia

Hematological parameters were studied for 13 control rats, 17 ECM and 22 NoECM rats. We analyzed the impact of K173 infection on red and white blood cells and platelet counts.

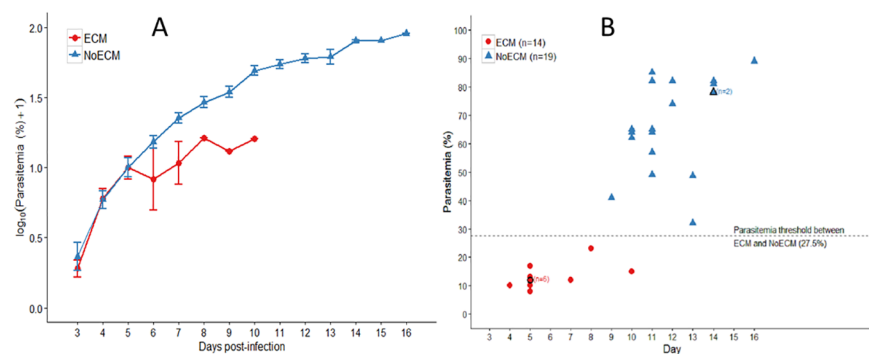


Fig 2. Parasitemia analysis. **A)** Parasitemia (Log%+1) in Sprague Dawley rats infected by K173. Young SD rats 4.5 weeks old were infected with $5 \cdot 10^7$ parasitized mouse erythrocytes by ip injection. Parasitemia determined from Giemsa stained tail blood smears was monitored from day 3 *pi*. Parasitemia in ECM and NoECM is presented versus days post-infection. Parasitemia is expressed in mean \pm standard error (SEM). **B)** Distribution of ECM (n = 14) and NoECM (n = 19) rats versus parasitemia at the day of the death. Some rats died very early on the morning and their last reported parasitemia dated from the previous evening explaining why some points have one-day difference between Fig 1 and Fig 2B. There was no overlap of the two populations leading to a parasitemia threshold of 27.5% being established allowing the prediction that over this value all infected rats will not display a CM event but severe anemia.

<https://doi.org/10.1371/journal.pone.0181300.g002>

Red Blood Cells (RBCs): The RBCs, hemoglobin and hematocrit levels were analyzed to assess anemia (Fig 3 and S1 Table). The progression of RBC counts during the course of infection (Fig 3A) showed that ECM rats presented a stable RBC count remaining at the level of the controls but was significantly different with NoECM ($p = 0.036$). From D+2 (2 days after the point when parasitemia was estimated at 5%) (S1B Fig), RBC count in the NoECM group decreased gradually as a function of parasitemia ($r = 0.75$, $p < 0.001$). For control rats, day D corresponds to Day 5 after the beginning of the experiment. Hemoglobin (HGB) ($p = 0.005$) and hematocrit (HT) ($p = 0.026$) also displayed the same trends between ECM and NoECM groups (Fig 3B and 3C, respectively). The decrease of these 3 parameters only in NoECM rats attested to the progression towards severe anemia while the stability at the control level was associated with a high risk of ECM. This result revealed that ECM occurrence in SD rats was not associated to anemia. However Muller *et al.* [42] established that anemia was not associated with the frequency of malaria episodes in children, nor with malaria prevalence but was significantly associated with malnutrition. Indeed, malaria, anemia and under-nutrition are 3 diseases frequently co-existing in children aged less than 5 years in the sub-Saharan endemic area [43] explaining that CM in children, commonly presenting anemia [44].

The Mean Corpuscular Volume (MCV) (Fig 4A), the Mean Corpuscular Hemoglobin Concentration (MCHC) (Fig 4B), the Mean Corpuscular Hemoglobin (MCH) (S3A Fig), and the Red Cell Distribution Width (RDW) (S3B Fig) were used to characterize the type of anemia affecting the NoECM rats. In ECM rats, MCV remained stable over time of infection and comparable to control values while in anemic NoECM rats, MCV increased gradually highlighting an increase of RBC volume corresponding to a strong arrival of young reticulocytes in the blood flow (reticulocytosis) (Figs 4A and S3B). The utility of a reticulocyte count only appeared after data analysis, explaining why it was not carried out during blood analysis. However, we can assume that the MCV increase implies macrocytic and regenerative anemia. From D+3, the MCV was significantly higher in NoECM compared to control rats ($p = 0.015$). The MCHC values likewise remained stable in NoECM rats until D+3 but then decreased compared to control rats ($p = 0.001$) indicating a shift from normochromic to hypochromic anemia (Figs 4B and S3A; S1 Table).

The follow-up of anemia parameters such as MCV, MCHC, MCH and RDW were in accordance with the RBC count, hemoglobin and hematocrit levels and showed that they clearly discriminated ECM from NoECM rats (S2 Fig). Anemia is a constant feature of malaria infection. Pregnant women mostly primigravidae and children below the age of 5 years are the most afflicted. Anemia pathogenesis is multifactorial and incompletely understood. Among several

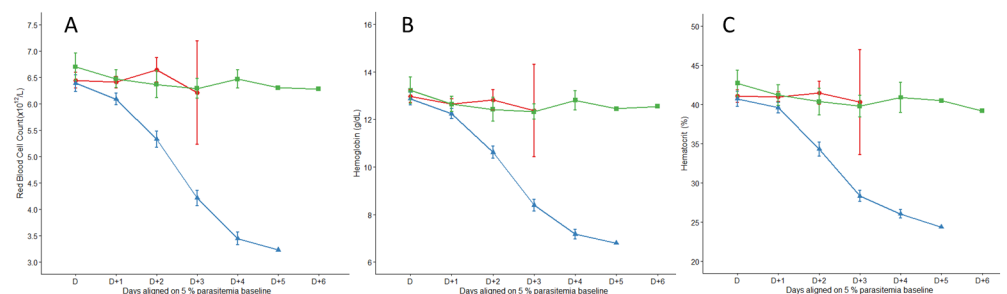


Fig 3. Blood parameters analysis. Red blood cells (RBCs) (A), hemoglobin (HGB) (B) and hematocrit (HT) (C) in ECM ($n = 17$), NoECM ($n = 22$) and control ($n = 13$) groups during K173 infection. The hematological parameters are aligned from and on the basis of day (D) where parasitemia was estimated at 5% (S1B Fig). Hemoglobin and hematocrit also displayed same trends between ECM and NoECM groups (3B and 3C). All data are represented by mean \pm standard error of the mean (SEM).

<https://doi.org/10.1371/journal.pone.0181300.g003>

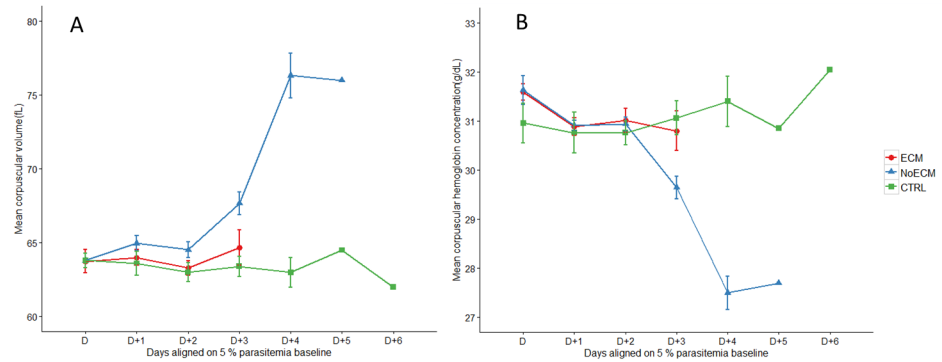


Fig 4. Hematological parameters in the course of infection in ECM (n = 17), NoECM (n = 22) and control (n = 13) groups. Mean Corpuscular Volume (MCV) (A) and Mean Corpuscular Hemoglobin Concentration (MCHC) (B) kinetics. The hematological parameters are aligned from and on the basis of the day (D) when parasitemia was estimated at 5% (S1B Fig). All data are represented by mean ± standard error of the mean (SEM).

<https://doi.org/10.1371/journal.pone.0181300.g004>

factors, the destruction of erythrocytes (RBCs) and the removal of non-parasitized RBCs in acute malaria are the most frequently observed causes of severe malarial anemia [45].

Platelets: Platelet count (Fig 5A), Mean Platelet Volume (MPV) (Fig 5B) and the Platelet Distribution Width (PDW) (S4 Fig) were analyzed to characterize the impact of K173 infection on SD rat platelets (S1 Table). A drastic decline of platelet count was observed over time in infected rats (ECM and NoECM) compared to control ($p < 0.001$) (Fig 5A). This thrombocytopenia was inversely proportional to the parasitemia ($r = 0.82$, $p < 0.001$) but no significant difference of platelet counts was observed between ECM and NoECM groups ($p = 0.496$) indicating a simple link between thrombocytopenia and K173 infection. The MPV parameter study presented a similar increasing trend in all infected groups (Fig 5B). The increased MPV values reflect the augmentation in the bloodstream of the number of young platelets, which are larger than old platelets. This indicates that the thrombocytopenia in infected rats was peripheral because it was regenerative and may thus be due to strong platelet consumption. This phenomenon is similar to platelet patterns in Human severe malaria especially in children [39,46–50].

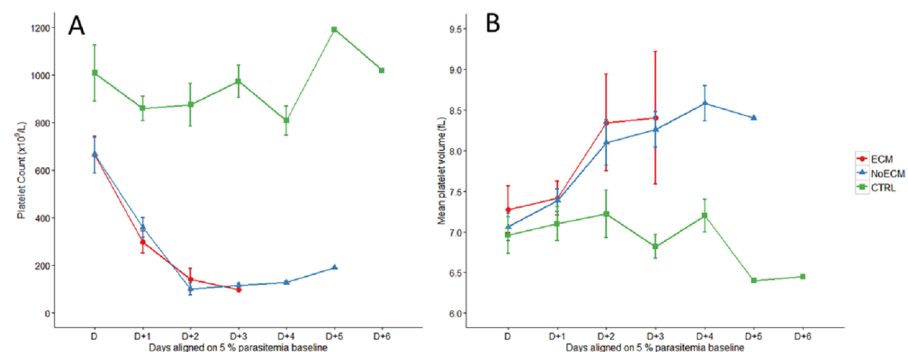


Fig 5. Hematological parameters in the course of infection in ECM (n = 17), NoECM (n = 22) and control (n = 13) groups. Platelet counts (A) and Mean Platelet Volume (MPV) (B). The hematological parameters are aligned from and on the basis of the day (D) when parasitemia was estimated at 5% (S1B Fig). All data are represented by the mean ± standard error of the mean.

<https://doi.org/10.1371/journal.pone.0181300.g005>

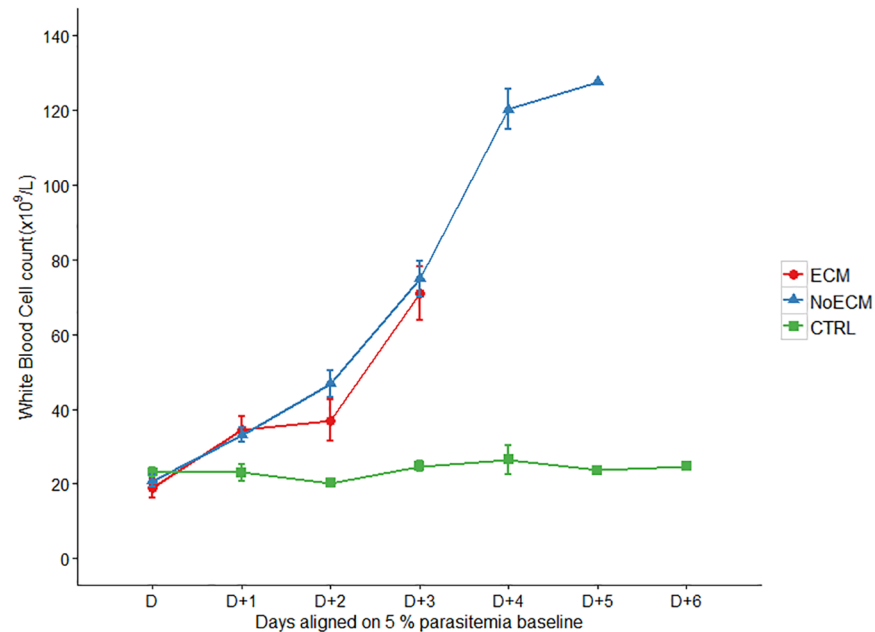


Fig 6. White blood cell count during the course of infection in ECM (n = 17), NoECM (n = 22) and control (n = 13) groups. Parameters are aligned from and on the basis of the day (D) where parasitemia was estimated at 5% (S1B Fig). All data are represented by the mean \pm standard error of the mean (SEM).

<https://doi.org/10.1371/journal.pone.0181300.g006>

White Blood Cells (WBCs): The total and differential leucocyte counts were significantly increased during K173 infection compared to the control group. This count was correlated to following the parasitemia but no difference between ECM and NoECM rats was observed (Figs 6 and S2; S1 Table). This increase mainly concerned lymphocytes (S5C Fig), granulocytes (S5A Fig) and less but still significantly monocytes (S5B Fig). This leukocytosis including lymphocytosis and monocytosis was in accordance with observations in children suffering from falciparum malaria, for whom high levels of lymphocytes were reported [50].

ECM in SD rats leads to multivisceral deficiencies

Because of the great variations in parasitemia in the NoECM group, the NoECM rats were split into 2 cohorts of differing parasitemia level. Group 1 had a lower parasitemia (NoECM_{LP}: mean parasitemia = 26.5% \pm 2.25; n = 4) close to the parasitemia of ECM rats (mean 21.8% \pm 2.6; n = 6), (p = 0.218) and Group 2 presented hyperparasitemia (NoECM_{HP}: mean parasitemia 61.4% \pm 3.3; n = 9), (p < 0.001). Among all biochemical parameters measured (Fig 7 and S2 Table), ECM rats presented a significant increase of creatinine levels (p = 0.001) and a significant decrease of glycemia (p = 0.037) and total CO₂ (p < 0.001) compared to the control group. The same was observed in NoECMs. High levels of creatinine, observed principally in ECM and NoECM_{HP} rats, have also been reported in children suffering of CM in Africa where hypercreatinemia was reported to be a risk factor of mortality [37,51]. This increase could be linked to renal failure also described in severe malaria [2,52].

A significant decrease of total CO₂ level (p < 0.001) observed in ECM rats compared to control was probably a sign of metabolic acidosis. Generally, serum bicarbonate accounts for about 95% of the total CO₂ content; thus the measurement of total CO₂ is an excellent estimator of serum bicarbonate [53]. The lower levels of total CO₂ result from metabolic acidosis which is one of WHO criteria of severe malaria (plasma bicarbonate

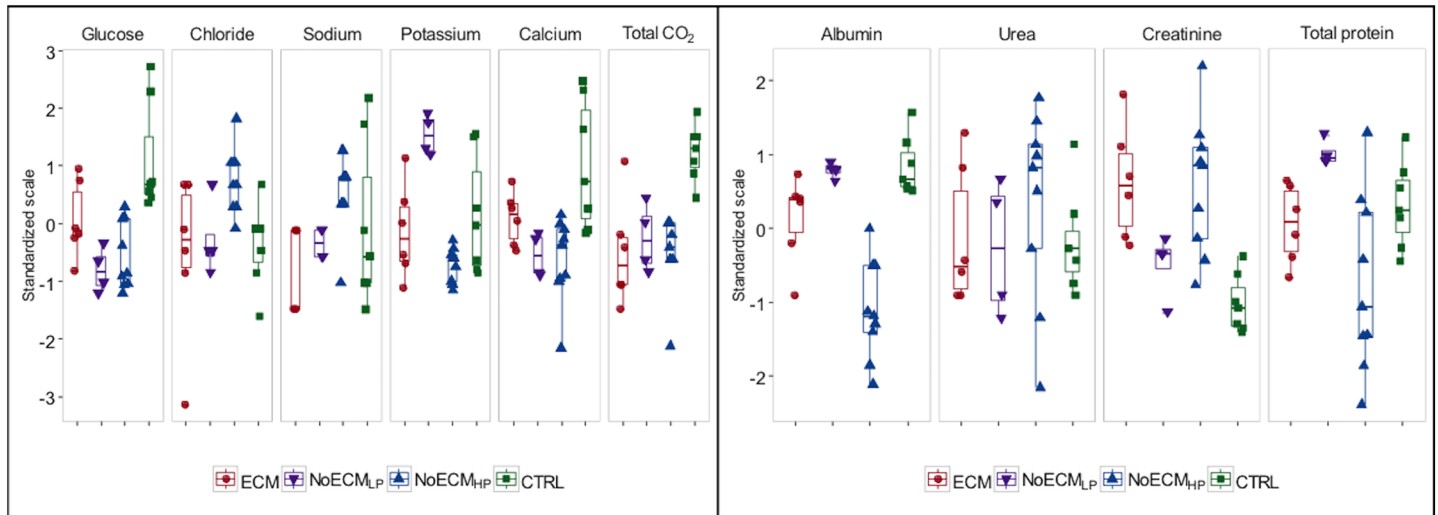


Fig 7. Biochemical parameters of SD rats infected by K173. Globally significant differences between ECM, NoECM and control (CTRL) groups were observed for creatinine ($p = 0.001$) potassium ($p < 0.001$) glycemia ($p < 0.001$), calcium ($p = 0.002$), albumin ($p < 0.001$) and total CO_2 ($p < 0.001$). The ECM group was significantly different from the CTRL group for creatinine ($p = 0.001$), glucose ($p = 0.037$) and total CO_2 ($p < 0.001$), from the NoECM_{LP} group only for potassium ($p = 0.004$) and from the NoECM_{HP} group for albumin ($p = 0.001$) and chloride ($p = 0.0029$). To suppress the influence of parameter units, the data are plotted on a standardized scale, e.g. mean = 0 and SD = 1.

<https://doi.org/10.1371/journal.pone.0181300.g007>

concentration $< 15\text{mmol/L}$ [4]. Acidosis is currently observed in CM children and is considered predictive of death [54]. However, the diagnosis of metabolic acidosis is made by arterial blood gas analysis. The low CO_2 levels in venous blood here reported is thus suggestive; for definitive diagnosis an arterial-blood gas would be needed.

The low glucose levels reported in ECM rats followed a trend similar to that of hypoglycemia observed globally in CM in children [44,55]. Indeed, hypoglycemia (blood glucose $< 2.2\text{mmol/L}$) is particularly common in children less than 5 years old, especially when seizures, coma or hyperparasitemia occur. In some cases of pernicious falciparum malaria, hypoglycemia less than 0.4g/L was associated to higher mortality rates [56]. However, as also observed in our study model, hypoglycemia is not a specific complication of CM but is found in severely ill fasted children, resulting from glycogen depletion and/or possibly impaired hepatic gluconeogenesis [57].

Albumin levels also presented a decrease for ECM rats compared to control rats. However, even though a significant difference ($p = 0.001$) was reported between the ECM and NoECM_{HP} groups, the same trend was observed between ECM and controls ($p = 0.073$). Total proteins showed the same variation as albumin. The decrease in serum albumin / total proteins indicated that severe forms of K173 infection in SD rats lead to electrolyte imbalance reflecting renal and/or hepatic failure. Hypoalbuminemia in ECM and NoECM_{HP} groups associated to hypercreatinemia in the same groups, confirmed renal impairment as reported in human severe malaria including CM [58,59].

Surprisingly, potassium was significantly higher in NoECM_{LP} rats than in ECM ($p = 0.004$), NoECM_{HP} and control rats. Hyperkalemia is reported in children with severe malaria especially with CM [59,60]. Hyperkalemia can complicate acidosis and can increase the risk of mortality [60]. Excess potassium levels can result from acute renal failure [59] or potassium moving out of its usual location within cells into the bloodstream including destruction of red blood cells (hemolysis). This difference between anemic NoECM_{HP} rats and NoECM_{LP} could result from a lower number of RBCs being present and elimination of circulating potassium.

Globally biochemical analysis revealed that in SD rats K173 infection could lead to acute renal failure during ECM while, in NoECM_{HP} rats, a chronic renal failure was noted which can be associated to a hepatic failure. NoECM_{LP} which is a milder form of malaria presented less renal impairment than ECM and NoECM_{HP}. The impact of K173 infection in this model is close to that observed in human malaria [52,59,61,62]. Hypoglycemia, acidosis and renal failure observed in this rat model are the main WHO criteria to define severe forms of malaria [4]. The SD rat model thus appears as particularly relevant to study the impact of malaria in Human CM multivisceral deficiencies.

Cytokine expression profile in K173-infected rat

For a better understanding of the cytokine profiles of ECM in SD rats infected by K173, brain cytokine gene expression was analyzed in ECM (n = 14), NoECM (n = 23) and Control (n = 7) brains. Among the 12 brain cytokine gene expressions assessed, INF γ (p<0.001), IL10 (p<0.001), MIP1 β (p<0.001), IL1 β (p = 0.001), TNF α (p = 0.045), and MIP1 α (p<0.014) were significantly up-regulated in all parasitized rats compared to the control group (Figs 8 and S6; S3 Table). IL12p40 mRNA was significantly up-regulated only in the NoECM group compared to the control group (p = 0.04). Comparison of ECM with NoECM rats showed that IL10 mRNA levels were up-regulated more in ECM rats than in NoECM rats (p = 0.044) and TGF β mRNA expression had a greater trend towards up-regulation in NoECM than ECM groups (p = 0.073). The study of IL10:TNF α level ratios showed that severe malaria cases (grouped data from both ECM and NoECM rats) are significantly lower than controls (p = 0.001). These data from cerebral cytokines are in accordance with plasma level ratio already reported in Humans [63].

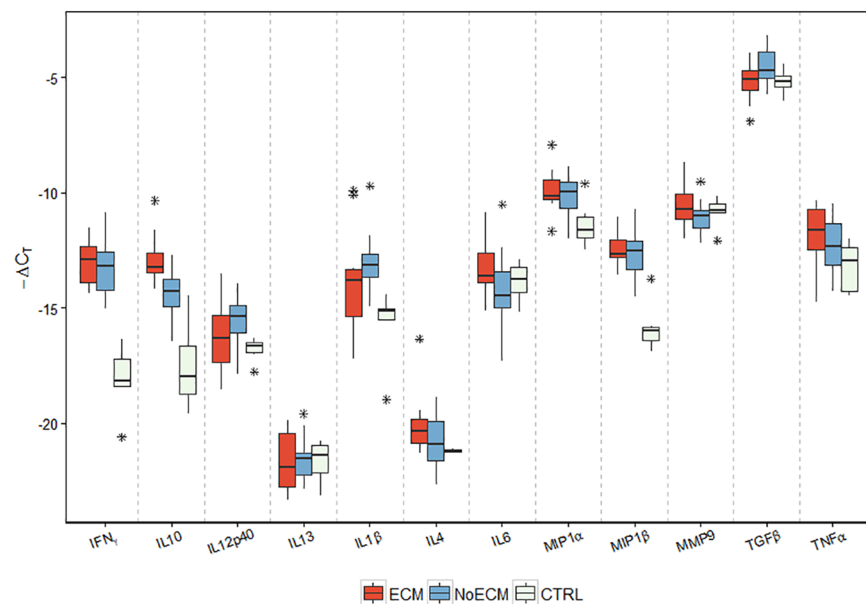


Fig 8. Expression of cytokines in SD rat brains infected by K173. Cerebral cytokine gene expression was assessed in ECM (n = 14), NoECM (n = 23) and Control brains (n = 7). Samples were collected on day ECM onset for ECM rats, after the parasitemia reached 30% for NoECM rats and for control rats at the same time as ECM and NoECM groups. Box plots represent medians and 25th and 75th percentiles. Among all the cytokines investigated only the gene expression of INF γ (p<0.001), IL10 (p<0.001), IL1 β (p = 0.001), TNF α (p = 0.045), MIP1 α (p<0.014) and MIP1 β (p<0.001) were significantly different between infected and control rats. The symbol * indicates outliers.

<https://doi.org/10.1371/journal.pone.0181300.g008>

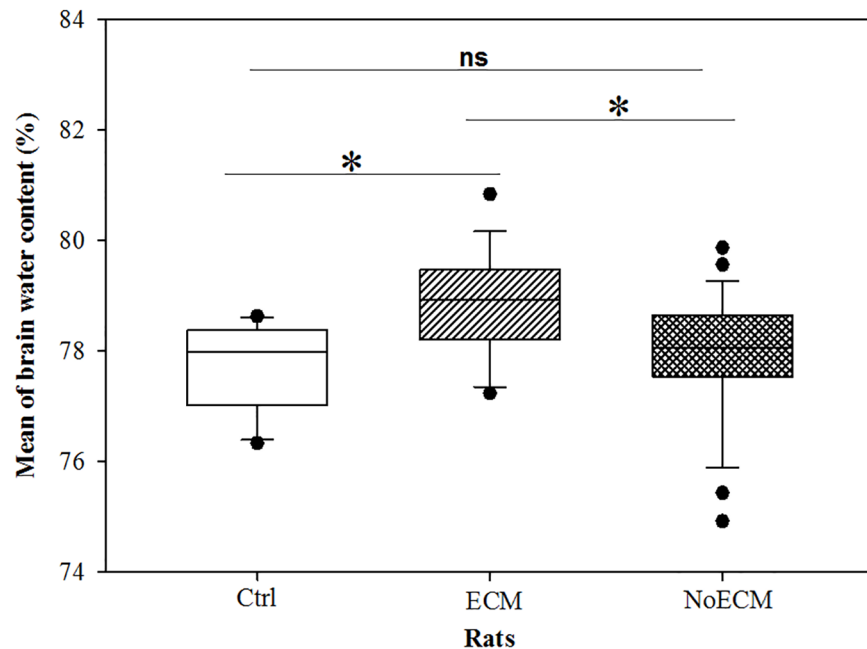


Fig 9. Edema test. Quantification of water contained in brains of ECM (n = 12), NoECM (n = 13) and Control brains (n = 8). The brain water content in the ECM group was statistically higher than that in NoECM (p = 0.007) and Control rats (p = 0.02). The p value was not significant (ns) between NoECM and Control rats (p = 0.66). Box plots represent medians and 25th and 75th percentiles. Statistical test used: Kruskal-Wallis One Way Analysis of Variance on Ranks and Donn's Method for all pairwise comparisons. *p<0.05.

<https://doi.org/10.1371/journal.pone.0181300.g009>

The overexpression of TNF α , IFN γ , IL1 β , MIP1 α and MIP1 β genes in both ECM and NoECM rats suggest that the variations of these cytokines were linked to the infection. MIP1 α is involved in acute and chronic immune response against *P. falciparum* and its high levels may also cause anemia [64]. Local production of TNF α mRNA in the central nervous system plays a role in fatal murine ECM pathogenesis [65,66]. In Humans, a higher level of local production of TNF α mRNA in the central nervous system is associated to CM in children [67]. The involvement of TNF α in association with pro-inflammatory cytokines like IL1 β and TGF β was also reported in the Human CM immune response [68]. Decreased expression of TGF β associated with increased IFN γ expression has been reported in ECM in CBA/J mice [65].

Higher levels of IL10 have been previously reported in cerebral and severe human malaria compared to mild malaria [69,70]. IL10 is an immunoregulatory cytokine that has a critical role in downscaling the immune response to pathogens to prevent host damage and high expression levels of IL10 may induce immunodeficiency as found in some parasitic and retroviral infections in humans [71]. Conversely, IL10 seems to have a neuroprotective role in ECM in mice [72–74].

Brain cytokine gene expression in the present study was not significantly different between ECM and NoECM rats except for IL10. Nevertheless, the cytokines involved in this rat model (INF γ , IL10, TGF β , IL12p40, IL1 β , TNF α , MIP1 α , and MIP1 β) were similar to those reported in the immune malaria response [67,68] and in ECM mouse malaria [65,66].

Brain vascular permeability is altered during ECM in SD rat

Autopsies of ECM rats showed brain swelling compared NoECM and controls. The brain water content in the ECM group was higher than in NoECM (p = 0.007) and controls (p = 0.02) groups (Fig 9). No significant difference was noted between NoECM and Control

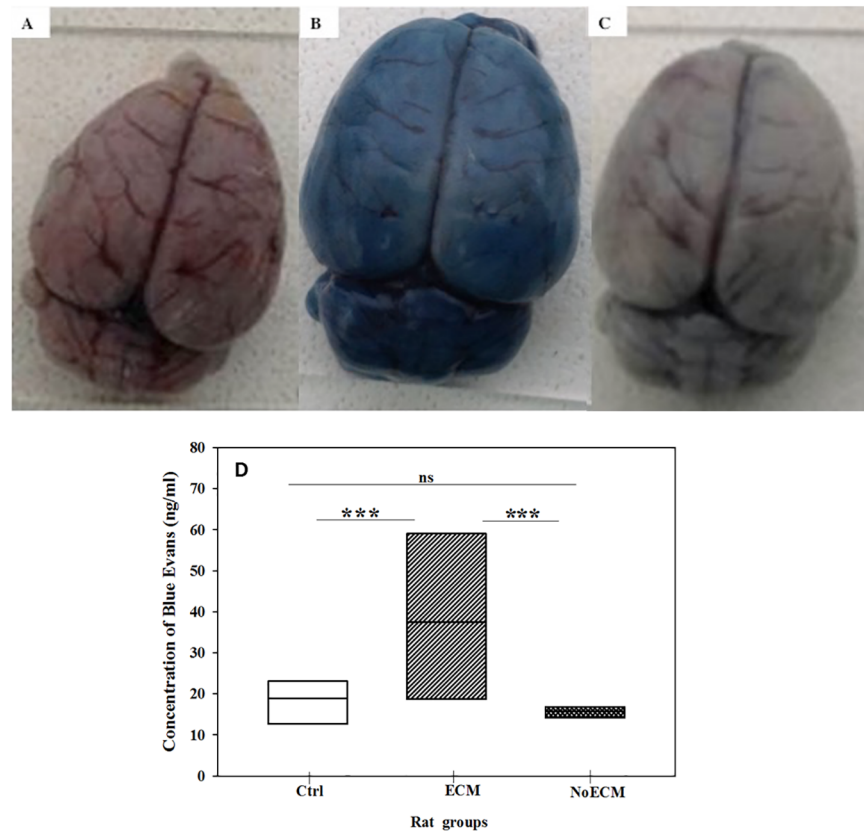


Fig 10. Assessment of brain vascular permeability. (A) Dorsal view of brain from Control (Ctrl), (B) Dorsal view of brain from ECM, and (C) Dorsal view of brain from NoECM rats after injection of Evans blue dye in tail vessel and sacrifice 90 minutes later. (D) Quantification of Evans blue dye concentration in brain of non-infected (Control; $n = 7$) and infected rats (ECM; $n = 5$ or NoECM; $n = 8$). After Evans blue dye injection, brain was removed and immersed in a 2 ml of paraformaldehyde (PFA) for 48h at 37°C. The extravasated dye was quantified by spectrophotometer. Box plots represent medians and 25th and 75th percentiles. Statistical test used: Kruskal-Wallis One Way Analysis of Variance on Ranks and Donn's Method for all pairwise comparisons. * $p < 0.05$; ** $p < 0.005$; *** $p < 0.001$.

<https://doi.org/10.1371/journal.pone.0181300.g010>

rats ($p = 0.66$). The brain swelling and the increased water content indicate altered vascular permeability. These data were confirmed by the analysis of a significant difference in tissue extravasations of Blue Evans dye between in ECM, NoECM and control brains ($p = 0.028$) (Fig 10B, 10C and 10A, respectively). More Evans Blue was detected in brains from ECM rats than NoECM meaning an increase of the blood brain barrier (BBB) permeability during ECM (Fig 10D). This result supports the role of BBB loss of integrity in the cerebral edema.

Brain swelling, also reported in the ECM mouse model [75–77], is a common feature of Human CM in adults [78–80] and African children [36,81–84]. The computed tomographic scans of Human CM children with severe intracranial hypertension often showed ischemic lesions [85,86]. The mechanisms responsible for the dysfunction of the BBB in Human CM have not been completely elucidated but adhesion of sequestered infected red blood cells (iRBCs) to cerebral endothelium has been proposed as a contributing factor [80,86]. Moreover the role of cerebral edema in the pathophysiological features and the clinical outcome of Human CM is not well understood and remains controversial [78,87]. Indeed, autopsies of adult Human CM patients have shown that brain swelling is not always present which does not support a direct link between brain swelling and a fatal outcome [78,88].

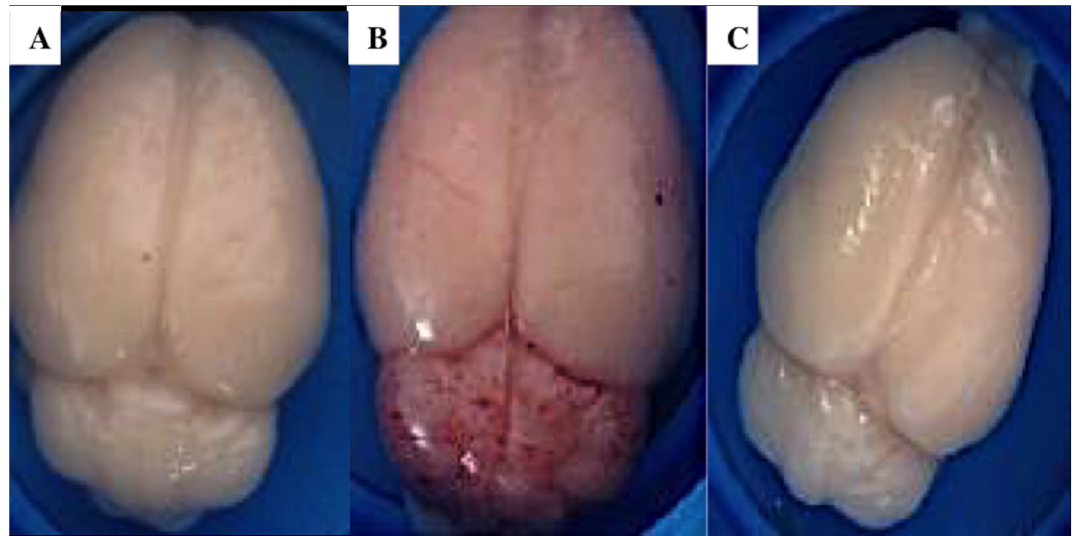


Fig 11. Dorsal view of brains from K173 infected SD rats after systemic lavage. (A) Healthy brain of a Control (Ctrl) rat. (B) ECM brain shows petechial hemorrhages especially on cerebellum and edema with disappearance of cerebral longitudinal fissure. (C) NoECM brain presents no macroscopic lesion.

<https://doi.org/10.1371/journal.pone.0181300.g011>

ECM in rats is associated to brain hemorrhages and sequestration in cerebral microvasculature

Gross examination of ECM ($n = 12$) brains showed an increased volume (ventriculomegaly) which is an obvious sign of brain swelling and petechial hemorrhages under the meninges on both cerebral hemispheres, more especially on the cerebellum (Fig 11B). By contrast, brains of NoECM rats ($n = 16$) had no macroscopic lesions (Fig 11C). The lesions are similar to those reported in autopsies of Human CM patients including a grey discoloration of the brain substance, petechial hemorrhages, predominantly in the white matter and cerebellar folia [2,38, 86,89]. Before systemic lavage, NoECM rats showed no brain hemorrhagic lesion but a discoloration, sign of symptomatic severe anemia, in comparison with control and ECM rats. After systemic lavage, No-ECM brains were comparable to Controls (Fig 11A) with no observed lesions.

In the ECM group, hemorrhages were mainly observed in brainstem and cerebellum on peri-meningeal and peri-ventricular areas in white and gray matter (S5 Table). The histological slices of ECM brain showed acute perivascular and neuropilar hemorrhages with severe extension associated with interstitial edema (Fig 12A). The hemorrhagic lesions were severe and extended in brain matter (Fig 12B). Numerous parasites were observed in hemorrhagic lesions (Figs 12C, 12D, 13C and 13D). Thrombosis was present in meninges and parenchyma (Fig 13A). Gliosis and neurophagia, with varying degrees of severity, were also observed in ECM and NoECM rats (S5 and S6 Tables). A large deposit of iRBCs was observed in micro-vessels of all infected rats mainly in NoECM rats (S5 Table). In ECM brains, parasites were particularly localized in direct contact of vessels walls raising the question of sequestered parasites (Fig 13). A systemic brain lavage to drain out blood stasis allowed us to clearly report parasite sequestration (intravascular and/or adhesion in micro-vessels) in all ECM brains (Fig 14D and 14E and S6 Table). By contrast, no macroscopic lesions were noted and iRBCs were totally absent in micro-vessels for any NoECM brains (Fig 14B) as Control brain (Fig 14A) after brain lavage, and despite hyperparasitemia in excess of 30%.

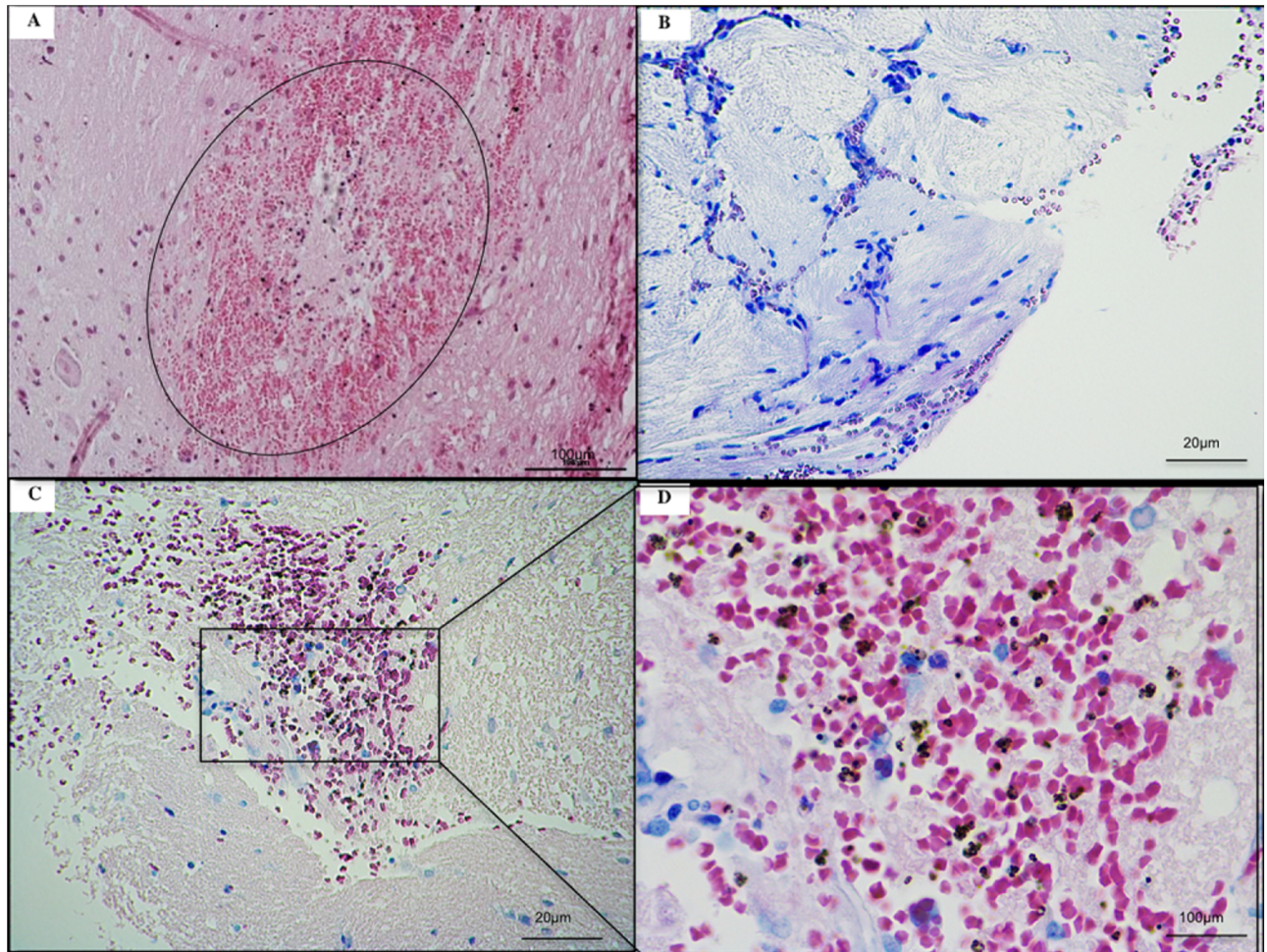


Fig 12. Histological illustrations of cerebral lesions in ECM K173 infected SD rats. (A) Acute perivascular neuropilar hemorrhage with severe extension (circle). Diffuse intracerebral hemorrhages (B and C) with presence of numerous parasites (D). ECM brains were collected from rats without systemic lavage. Histological slices of ECM brains stained using hematoxylin-eosin.

<https://doi.org/10.1371/journal.pone.0181300.g012>

Before systemic lavage, NoECM rats showed no brain hemorrhagic lesion but a discoloration, sign of symptomatic severe anemia, in comparison with control and ECM rats. After systemic lavage, NoECM brains were comparable to Controls with no observed lesions.

These results suggest that the sequestration of iRBCs in cerebral micro-vessels, considered as one of the main factors of Human CM occurrence [2,36,89], is observed in all ECM rats in the present model. Moreover, washing of the blood circulatory system is a robust technique which enables removing all ambiguity between adherent iRBCs and iRBCs in blood stasis. Therefore the present ECM rat model seems a relevant model of human CM. In ECM mouse models, even though iRBC sequestration can be reported, sequestered cells are essentially leukocytes [13,90,91,92].

Conclusion

The present experimental model of cerebral malaria in young Sprague Dawley rats infected by K173, appears as a particularly relevant model regarding the histological, physiological and biochemical parameters compared to those observed in Human CM. The most remarkable

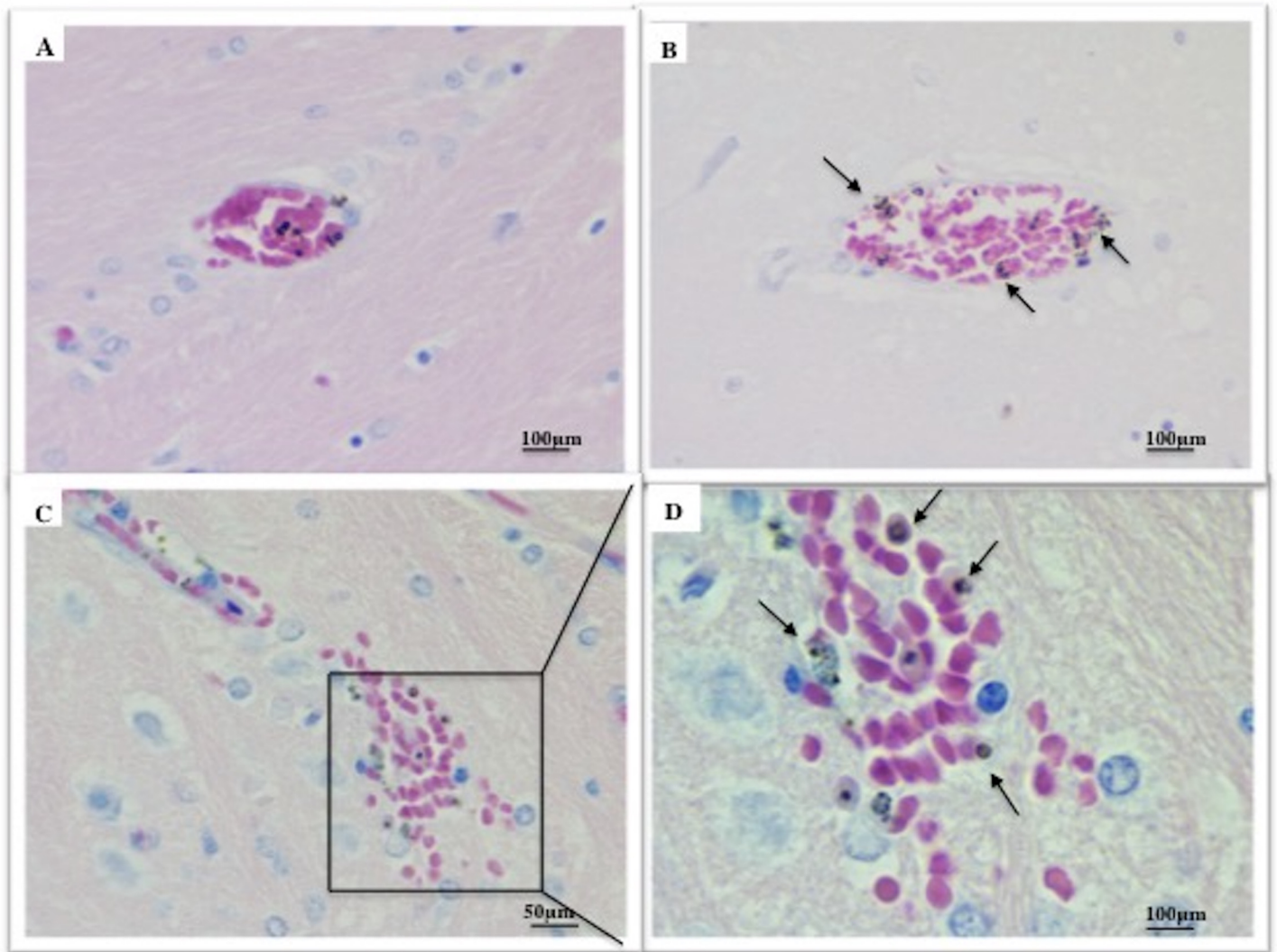


Fig 13. Localization of parasites in cerebral vessels in ECM K173 infected SD rats. (A) Thrombosis. (B) Parasites were localized in peripheries of cerebral vessels in direct contact with the endothelium. (C and D) Extravascular hemorrhage with parasites (arrows) localized in peripheries. ECM brains were collected from rats without systemic lavage. Histological slices of ECM brains stained using hematoxylin-eosin.

<https://doi.org/10.1371/journal.pone.0181300.g013>

point is the sequestration of iRBCs in brain micro-vessels in all ECM rats like in Human CM whereas this phenomenon is debated in the mouse model [13,93]. In this rat model, hematological parameters susceptible to be predictive of the ECM progression were also determined. The parameters most affected in the ECM group were platelets and white blood cells with regenerative thrombocytopenia and leukocytosis as observed in Human CM while RBC count remained normal. It would be of great interest to determine whether the RBCs associated with hematocrit and hemoglobin, during the hospitalization of patients affected by malaria could be used to predict severe outcomes. In Human CM, it is urgent to stop and to reverse the development of symptoms, as quickly as possible, because of the high risk of neurological sequelae. Even though artemisinin-based therapies decrease parasitemia rapidly, the neuropathology also needs to be treated, perhaps by an adjunct therapy associated to the antiparasitic compound. For the moment none of the compounds tested (for instance: protein C, ADAMTS 13 protease activator, nitric oxide, angiotensin-II inhibitor, erythropoietin) has a real protective

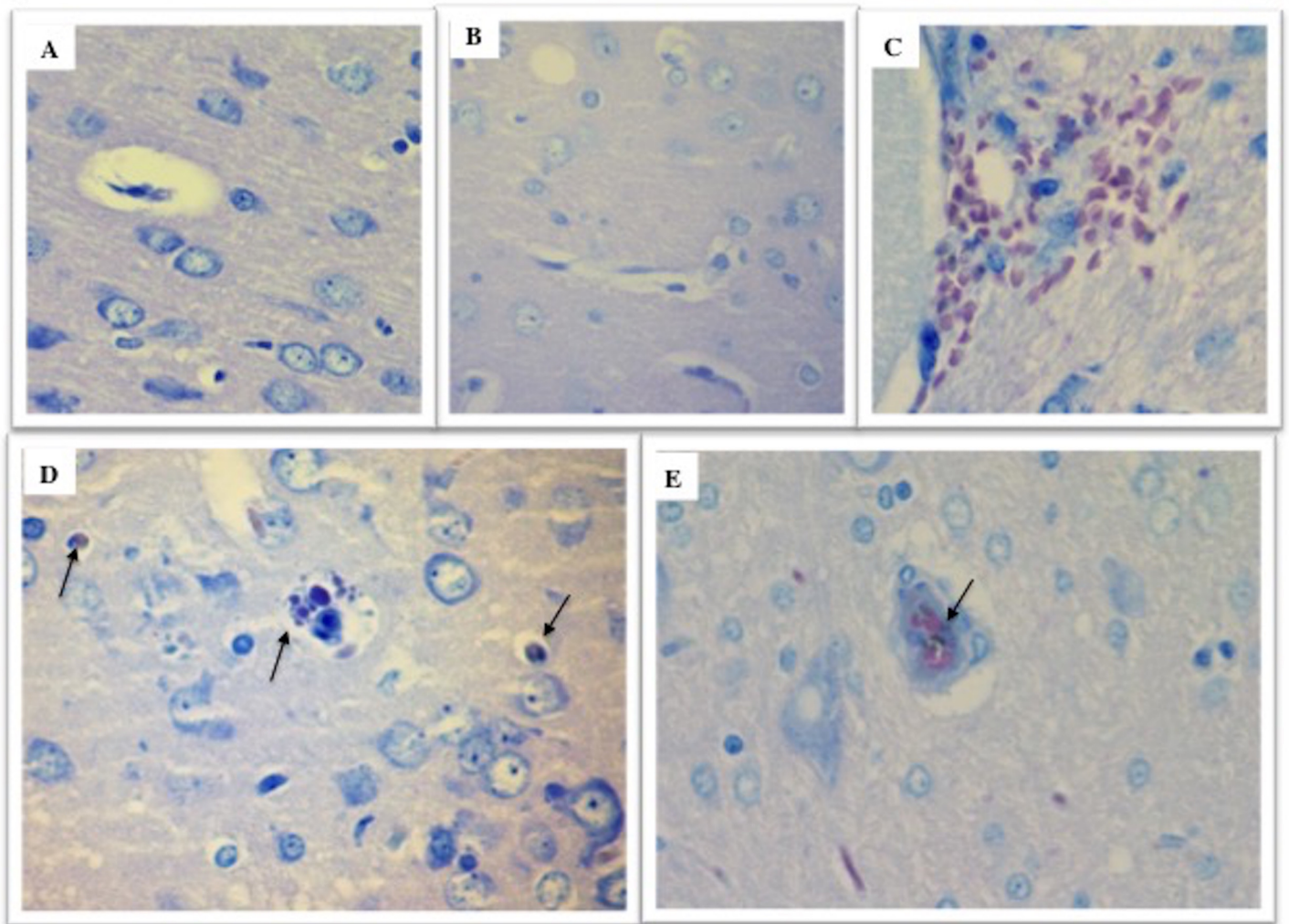


Fig 14. ECM in SD rats is associated with sequestration of infected red blood cells. Systemic lavage cleans out blood in micro-vessels. Parasites and lesions were totally absent in micro-vessels of Control (A) and NoECM brains (B). However in ECM brains, hemorrhagic lesions persist (C) and parasites were still present in micro-vessels (arrows) (D and E). Histological slices of ECM brains stained using hematoxylin-eosin.

<https://doi.org/10.1371/journal.pone.0181300.g014>

action against the deleterious effects of Human CM [4]. The present ECM rat model is thus an interesting tool in the search for such molecules in a relevant pharmacological approach.

Materials and methods

Ethics statement

All animal care and experimentation was performed according to European regulations (directive 86/609/EEC revised by the new directive 2010/63/UE) and approved by the French Institutional Animal Experimentation Ethics Committee (approvals MP/02/02/01/08, MP/03/02/01/08, MP/01/35/04/12, and 2016041515469392). The experiments were carried out in the animal facility of the Ranguel Hospital Department of Parasitology, Toulouse (France), under the control of the National Veterinary Services (accreditation N° B31 555 03). The staff in charge of the animal experiments received appropriate training and were granted a license delivered by the French Agricultural Ministry for experimentation on small laboratory animals.

Parasites

Plasmodium berghei Keyberg 173 (K173) murine strain of *Plasmodium*, was maintained in 6-week-old Swiss mice. The mice received 100 μ L of infected whole blood by intraperitoneal (ip) injection. Every five days, a new transfer of K173 parasites was performed from infected mice to healthy mice by the same process. K173 was transferred to rats between the 5th and the 25th mouse transfer [28].

Rats and infection

Male Sprague Dawley (SD) rats 4.5 weeks old were selected as animal model. They were supplied by Janvier Labs (Le Genest, Saint-Isle, France) placed 2 per cage and maintained under Specific Pathogen Free (SPF) conditions before experiments. The animals were acclimatized for 8 days and adapted to an artificial day-night rhythm of 12 h. Food and water were available *ad libitum*.

SD rats were inoculated at 4.5 weeks old by ip injection of 5.10^7 iRBCs collected from infected mice and diluted in 200 μ L of saline solution. From the 3rd day post-infection (*pi*), the monitoring of rats was performed every two hours (from 6:00 am to 10:00 pm) and all clinical signs were recorded.

Seven independent experiments were carried out for this study. The first was to evaluate parasitemia and clinical evolution and to define ECM and NoECM status, the second was to follow the hematological parameters and the third to study the biochemical variations. The immunological profiles of infected rats were also studied through by following cerebral cytokine gene expressions in two independent experiments. The impact of ECM in brain vascular permeability was evaluated by two other experiments: Evans blue test and edema test. Histopathological studies were performed to evaluate sequestration phenomena at the same time as cerebral cytokine evaluation.

Assessment of clinical evolution and definition of ECM and NoECM

To determine the survival rate and objective criteria for euthanasia to reduce animal suffering, 40 infected rats in two independent experiments were monitored without preliminary human intervention in order to follow clinical and parasitological evolution in a reference experiment of this experimental disease. However, during the entire experiment, a high vigilance about animal suffering problems was set up in order to minimize it. Each potential pain situation was assessed and kept to a minimum with two strict humane endpoints: parasitemia of rats superior to 80% and rats presenting coma. This preliminary experiment permitted to affine humane endpoints and then to euthanize animals earlier avoiding animal suffering. From 18 rats with ECM symptoms, 14 died without euthanasia because of the quick evolution of the disease and death within 12 hours.

The clinical progression in rats was evaluated by neurological assessment based on the animals' mobility. A diagnosis of ECM was made when infected rats presented neurological symptoms characterized, firstly, by paresis, followed by limb paralysis (right and/or left) and then total paralysis before coma. Data from this survival assay allowed accurate separation of a NoECM group, for animals without ECM, *i.e.* rats without any neurological signs but presenting parasitemia of over 23%. For analyses requiring the death of the rat (histopathological examinations, Evans blue dye assay, cerebral cytokine analysis and cerebral edema test), the rats were sacrificed in a CO₂ chamber at the presumed onset of objective symptoms of ECM or NoECM according to the above-mentioned definition. For assays with longitudinal monitoring (hematological, biochemical), classification into the ECM or NoECM groups was carried out *a posteriori*, according to the above definition.

Assessment of parasitemia

Parasitemia was determined daily from day 3 *pi*, by microscopic examination of tail blood smears after Giemsa staining. The kinetics of parasitemia was not only modulated by the time (*i.e.* days post-infection) but also by the inter-individual variability of the rats. Before 5% parasitemia, this kinetics of parasitemia varied greatly from one animal to another. Some rats reached 5% parasitemia four days *pi* while for others it took 6 to 8 days *pi*. After reaching 5% parasitemia the progression of parasitemia was similar for all infected rats. As the clinical status of infected rats may depend on the level of parasitemia, the results were analyzed not as a function of days post-infection but rather from a baseline set at 5% of parasitemia (day D) (S1B Fig). For control rats, the Day D corresponds to Day 5, *i.e.* the mean of the day D for 5% parasitemia after the beginning of the experiment.

Hematological parameters analysis

A 30 μ L-tail blood sample was taken from on each rat, 4 hours before infection, and then daily until day 3 *pi*. The blood was collected through micropipettes (Microvette[®], K2 EDTA, Sarstedt, France) and analyzed within 15 to 60 minutes. Daily hemograms were followed up during the timescale of the experiment. Estimation of hemoglobin content, hematocrit, red blood cell (RBC), white blood cell (WBC) and platelet count were performed by the hematologic analyzer (ABX MICROS-60-Diagnostics, Horiba ABX SAS, France). The differential WBC counts include granulocytes, lymphocytes and monocytes. Mean cell volume (MCV) indicates the volume of the average red blood cell and is expressed in femtoliters (fl). Mean cell hemoglobin (MCH) represents the absolute amount of hemoglobin in the average red blood cell in a sample and is expressed in picograms (pg) per cell. The MCH was calculated from the hemoglobin and the RBC data. Mean corpuscular hemoglobin concentration (MCHC) is the average amount of hemoglobin per deciliter of red cells (g/dl). The red blood cell distribution width (RDW) is a calculation of the variation in the size of RBCs. The mean platelet volume (MPV) was also measured.

Biochemical analysis

Animals were anesthetized with isoflurane and the blood collected from the retro-orbital sinus in dry plain tubes. Blood collection on ECM rats was completed as soon as clinical signs occurred. For NoECM the collection was carried out *a posteriori*, as defined above. The blood sampling was done on control rats at the same time as ECM and NoECM rats. Biochemical parameters including glucose, protein, albumin, creatinine, urea, total CO₂, sodium, potassium, chloride and calcium were measured on infected and control rats on the same blood samples by the Laboratoire Central de Biologie Médicale (LCBM)—ENVIT, Toulouse, France.

Brain quantitative real time PCR

Quantitative real-time PCR (RT-qPCR) was performed to determine the relative mRNA expression levels of TNF α , TGF β , IFN γ , MIP1 α , MIP1 β , MMP9, IL1 β , IL4, IL6, IL10, IL12p40 and IL13 genes in brain samples collected from rats ECM, NoECM and controls. Rats were euthanized by CO₂ at the presumed onset of objective symptoms of ECM or NoECM, brains were removed and immediately frozen in liquid nitrogen. Total RNA was isolated using Trizol reagent (Gibco-BRL, pays). RNA purification and DNase treatment were performed using respectively RNA easyminkits and DNA-free kits (Qiagen, Netherlands), according to the manufacturer's instructions. RNA concentration was evaluated by spectrophotometry at 260 nm. Reverse transcription of RNA was performed from 2 μ g for each sample using an iScript

cDNA synthesis kit (Bio-Rad Laboratories, pays). Real-time PCR assays were performed on 10 ng cDNA (RNA equivalent) in 25 μ L volume reaction per well using Power SYBR[®] Green PCR Master Mix as reporter dye, and the automated photometric detector ABI Prism 7000 Sequence Detection System for data acquisition (Applied Biosystems, France). The primers used are listed in [S4 Table](#). The geometric means of the threshold cycle (C_T) values of house-keeping genes (GAPDH) were used as the baseline for comparing the ΔC_T value [94].

Assessment of brain vascular permeability

Brain Water content [95]: a cerebral edema test was performed to assess the occurrence of edema during ECM. Rats were euthanized by CO₂ when clinical signs of ECM were observed. The brain was carefully removed, and weighed before and after being dried in a desiccating oven at 50°C for 72 h to obtain the dry weight. The same protocol was applied to NoECM and Control brains. The brain water content was calculated as follows:

$$\text{Water content (\%)} = [(wet\ weight - dry\ weight) \times 100] / wet\ weight.$$

Evans blue assay [96] was performed to evaluate the integrity of the BBB during ECM. 500 μ L of Evans blue dye (4%) was injected into tail veins of rats, once the clinical signs of ECM were observed. After 1 hour and half, rats were sacrificed by CO₂ and their brains collected and immersed in paraformaldehyde 4% at 37°C to extract the Evans blue dye. After 48h, the absorbance of the supernatant was measured in triplicates (100 μ L/well) at a wavelength of 630 nm using a BioTek ELISA spectrophotometer (Winooski, USA). Evans blue dye concentration (μ g/ml) was calculated using a calibration curve. In parallel, brains of NoECM and control rats were collected and treated with the same protocol.

Autopsy protocol and sample collection

Infected rats were sacrificed once clinical signs of ECM were observed or when the parasitemia reached 30% for NoECM rats. The rats were divided into 2 groups. In Group 1, the rats were anesthetized by muscular injection of a mix of Ketamine[®] and Xylazine[®] and then, after exsanguination, perfused by an intracardial injection of 180 mL of physiological serum to drain the systemic blood (BL for brain lavage) before removing the brains. In the second group, the rats were euthanized with CO₂ and the brains removed without lavage (NBL for No Brain Lavage). Macroscopic and histological examinations and immunological analysis were performed on both ECM and NoECM rats. Parasite adherence to brain micro-vessels was also evaluated.

Histopathological analysis

Collected brains (BL and NBL) were fixed in 4% paraformaldehyde and embedded in paraffin. Samples were dehydrated in Tissue processor HMP 110 (Microm Microtech, France), for 16 hours. Brain sections of 3–4 μ m were performed with a microtome, dried at 37°C for 30 minutes and stained with hematoxylin-eosin for microscopic examination. The sections were examined for hemorrhages and inflammation. Lesions were analyzed blind and classified from absence of lesion (-) to severe injury (+++++) according to their degree of severity.

Statistical analyses ([S1 Text](#))

On longitudinal assessments over the days, a 2-way analysis of the variance (or covariance in the case of baseline adjustment) with repeated measurements was performed. For end-point analyses, 1 or 2-way Analysis of Variance were used. *Post-hoc* tests for pairwise comparisons

were performed with Tukey's adjustment for multiplicity or Dunnett's adjustment for comparison to a referent group. Log transformation was applied for parameters underlying a Log-Normal distribution. As complementary analysis, Partial Least Square discriminant (PLS-DA) analyses were produced to describe the correlation structure of parameters dependent on the ECM/NoECM outcome. Data analyses were performed using "R: A language and environment for statistical computing" (R Core Team (2016)) and SAS/STAT® software 9.4 (SAS Institute Inc.).

For the Evans Blue and edema tests, the collected data were analyzed using SigmaPlot 11.0 software (Systat Software, Inc., San Jose California USA). Differences between all the experimental groups were analyzed by ANOVA and intergroup comparisons were made using the Holm-Sidak test. For parameters not having a normal distribution, the Kruskal-Wallis test followed by Dunn's post-hoc test was used. The level of $p \leq 0.05$ was considered statistically significant.

Supporting information

S1 Fig. Parasitemia analysis. **A)** Parasitemia (%) in ECM and NoECM rats *versus* time in days after infection. **B)** Parasitemia ($\text{Log}\%+1$) evolution in ECM and NoECM in function of days aligned on baseline parasitemia at 5%. **C)** $\log(\text{Parasitemia} + 1)$ evolution in Sprague Dawley rats infected by K173 with ECM ($n = 3$) and NoECM ($n = 3$), which survived after a total parasitic clearance. All data are represented by the mean \pm standard error of mean (SEM). (TIF)

S2 Fig. Discriminant analysis hematology. PLS-DA: Partial Least Square Discriminant Analysis is a supervised method designed to classify samples (here the Y class vector is ECM/NoECM) and identified the most predictive variables in the X-matrix of predictors. On actual values aligned DAY 2, performance of the fitting ("Leave-one-out" cross-validation method) gives an error rate of 28%. PLS-DA Hemato (CTRL excluded): error rate 28%. The distance between labels represents the correlation of parameters. The parameters are correlated with the closest class (ECM or NoECM). For example, high values for LY globally correspond to NoECM and low for ECM, while high values of RBC and superimposed parameters on the graph are associated with ECM. Red blood cell (RBC), white blood cell (WBC), platelet (Plt), granulocytes (GR), lymphocytes (LY), thrombocyte (THT), monocytes (MO), mean cell volume (MCV), mean cell hemoglobin (MCH), mean corpuscular hemoglobin concentration (MCHC), red blood cell distribution width (RDW), mean platelet volume (MPV). (TIF)

S3 Fig. Mean Corpuscular Hemoglobin (MCH) (A) and Red Cell Distribution Width (RDW) (B) during the course of K173 infection in ECM ($n = 17$), NoECM ($n = 22$) and Control (CTRL) ($n = 13$) groups. The hematological parameters are aligned from and on the basis of day D when parasitemia was estimated at 5% (S1B Fig). All data are represented by the mean \pm standard error of mean (SEM). (TIF)

S4 Fig. Evolution of Platelet Distribution Width (PDW) during the course of K173 infection in ECM ($n = 17$), NoECM ($n = 22$) and Control (CTRL) ($n = 13$) groups. The hematological parameters are aligned from and on the basis of the day D when parasitemia was estimated at 5% (S1B Fig). All data are represented by the mean \pm standard error of mean (SEM). (TIFF)

S5 Fig. Counts of granulocytes (A), monocytes (B) and lymphocytes (C) during the course of K173 infection in ECM (n = 17), NoECM (n = 22) and Control (CTRL) (n = 13) groups. Parameters are aligned from and on the basis of day D when parasitemia was estimated at 5% (S1B Fig). All data are represented by the mean \pm standard error of mean (SEM). (TIF)

S6 Fig. Discriminant analysis of cytokines (Delta CT) on Delta CT values. PLS-DA: Partial Least Square Discriminant Analysis is a supervised method designed to classify samples (here the Y class vector is ECM/NoECM) and identify the most predictive variables in the X-matrix of predictors. Performance of the fitting ("Leave-one-out" cross-validation method) gives an error rate of 13%. The distance between labels represents the correlation of parameters. The parameters are correlated with the closest class (ECM or NoECM) in the graph. For example, high values for IL10 and IL6 were globally high for ECM and low for NoECM rats. Other parameters, close to the centre or in the northwest quarter are globally not really informative for the discrimination as they are equidistant from ECM and NoECM. (TIF)

S1 Table. Hematological values of SD rats infected by K173 after the parasitemia reached 5% (Day D). Pairwise comparisons were performed with Tukey adjustment post-analysis of the covariance with repeated measurements on days D+1, D+2, D+3. (PDF)

S2 Table. Biochemical parameters of infected (ECM, NoECM) and control (CTRL) SD rats. NoECM rats were divided in 2 groups: NoECM_{LP} with lower parasitemia (mean parasitemia = 26.5%) close to the parasitemia of ECM rats (mean parasitemia = 21.8%), and NoECM_{HP} with hyperparasitemia (mean parasitemia = 61.4%). (TIF)

S3 Table. Cytokine expression analysis in brains from ECM, NoECM and control rats (global ANOVA is followed by post hoc test for pairwise comparisons with Tukey adjustment). (TIF)

S4 Table. List of genes and primer sequences used in RT-qPCR assays for cerebral cytokine analysis. (TIF)

S5 Table. Histological features of K173 malaria infected SD rats and Control rats in no brain lavage (NBL). (TIF)

S6 Table. Histological features of K173 malaria infected SD rats and Control rats after brain lavage (BL). (TIF)

S1 Text. Statistical analysis: Detail of tests used. (PDF)

Acknowledgments

We acknowledge Peter Winterton for editing the English, Hyphen-stat (Toulouse, France) to statistical analysis and Laurent Monbrun from the Phenotyping service—US006/CREFRE INSERM/UPS for his technical assistance.

Author Contributions

Conceptualization: Sokhna Keita Alassane, Marie-Laure Nicolau-Travers, Jean-Michel Augereau, Françoise Benoit-Vical.

Formal analysis: Sokhna Keita Alassane, Jean-Pierre Cambus, David Colongo, Jean-Michel Augereau, Françoise Benoit-Vical.

Funding acquisition: Françoise Benoit-Vical.

Investigation: Sokhna Keita Alassane, Marie-Laure Nicolau-Travers, Sandie Menard, Olivier Andreoletti, Noémie Gaudre, Sarah Abbes, Caroline Lacroux, Françoise Benoit-Vical.

Methodology: Sokhna Keita Alassane, Marie-Laure Nicolau-Travers, Olivier Andreoletti, Sarah Abbes, David Colongo, Jean-Michel Augereau, Caroline Lacroux, Xavier Iriart, Françoise Benoit-Vical.

Project administration: Françoise Benoit-Vical.

Resources: Françoise Benoit-Vical.

Supervision: Jean-Michel Augereau, Françoise Benoit-Vical.

Validation: Jean-Pierre Cambus, Myriam Wlodarczyk, Nicolas Blanchard, David Colongo, Babacar Faye, Jean-Michel Augereau, Caroline Lacroux, Xavier Iriart, Françoise Benoit-Vical.

Writing – original draft: Sokhna Keita Alassane, Jean-Michel Augereau, Françoise Benoit-Vical.

Writing – review & editing: Sokhna Keita Alassane, Marie-Laure Nicolau-Travers, Sandie Menard, Olivier Andreoletti, Jean-Pierre Cambus, Noémie Gaudre, Nicolas Blanchard, Antoine Berry, Sarah Abbes, David Colongo, Babacar Faye, Jean-Michel Augereau, Caroline Lacroux, Xavier Iriart, Françoise Benoit-Vical.

References

1. WHO. World Malaria Report 2015. 2015.
2. Idro R, Jenkins NE, Newton CRJC. Pathogenesis, clinical features, and neurological outcome of cerebral malaria. *Lancet Neurol*. 2005; 4: 827–40. [https://doi.org/10.1016/S1474-4422\(05\)70247-7](https://doi.org/10.1016/S1474-4422(05)70247-7) PMID: 16297841
3. Postels DG, Birbeck GL. Cerebral malaria. 1st ed. *Handbook of Clinical Neurology*. 2013, Elsevier B. V.; 2013. <https://doi.org/10.1016/B978-0-444-53490-3.00006-6>
4. World Health Organisation. Treatment of severe Malaria. Third WHO, editor. *Guidelines For The Treatment of Malaria*. 2015. 10.1016/0035-9203(91)90261-V
5. Birbeck GL, Beare N, Lewallen S, Glover SJ, Molyneux ME, Kaplan PW, et al. Identification of malaria retinopathy improves the specificity of the clinical diagnosis of cerebral malaria: Findings from a prospective cohort study. *Am J Trop Med Hyg*. 2010; 82: 231–234. <https://doi.org/10.4269/ajtmh.2010.09-0532> PMID: 20133998
6. Barrera V, Hiscott PS, Craig AG, White VA, Milner DA, Beare NAV, et al. Severity of retinopathy parallels the degree of parasite sequestration in the eyes and brains of malawian children with fatal cerebral malaria. *J Infect Dis*. 2015; 211: 1977–86. <https://doi.org/10.1093/infdis/jiu592> PMID: 25351204
7. Marsh K, Forster D, Waruiru C, Mwangi I, Winstanley M, Marsh V, et al. Indicators of life-threatening malaria in African children. *N Engl J Med*. 1995; 332: 1399–1404. <https://doi.org/10.1056/NEJM199505253322102> PMID: 7723795
8. Cox JA, Lukande RL, Katerregga A, Mayanja-Kizza H, Manabe YC, Colebunders R. Autopsy acceptance rate and reasons for decline in Mulago Hospital, Kampala, Uganda. *Trop Med Int Health*. 2011; 16: 1015–8. <https://doi.org/10.1111/j.1365-3156.2011.02798.x> PMID: 21564428

9. Langhorne J, Buffet P, Galinski M, Good M, Harty J, Leroy D, et al. The relevance of non-human primate and rodent malaria models for humans. *Malar J*. 2011; 10: 23. <https://doi.org/10.1186/1475-2875-10-23> PMID: 21288352
10. Grau GE, Mackenzie CD, Carr R a, Redard M, Pizzolato G, Allasia C, et al. Platelet accumulation in brain microvessels in fatal pediatric cerebral malaria. *J Infect Dis*. 2003; 187: 461–6. <https://doi.org/10.1086/367960> PMID: 12552430
11. Riley EM, Couper KN, Helmby H, Hafalla JCR, de Souza JB, Langhorne J, et al. Neuropathogenesis of human and murine malaria. *Trends Parasitol*. 2010; 26: 277–8. <https://doi.org/10.1016/j.pt.2010.03.002> PMID: 20338809
12. Rénia L, Grüner AC, Snounou G. Cerebral malaria: in praise of epistemes. *Trends Parasitol*. 2010; 26: 275–7. <https://doi.org/10.1016/j.pt.2010.03.005> PMID: 20363672
13. White NJ, Turner GDH, Medana IM, Dondorp AM, Day NPJ. The murine cerebral malaria phenomenon. *Trends Parasitol*. 2010; 26: 11–15. <https://doi.org/10.1016/j.pt.2009.10.007> PMID: 19932638
14. Craig AG, Grau GE, Janse C, Kazura JW, Milner D, Barnwell JW, et al. The role of animal models for research on severe malaria. *PLoS Pathog*. 2012; 8. <https://doi.org/10.1371/journal.ppat.1002401> PMID: 22319438
15. Mestas J, Hughes CCW. Of mice and not men: differences between mouse and human immunology. *J Immunol*. 2004; 172: 2731–2738. <https://doi.org/10.4049/jimmunol.172.5.2731> PMID: 14978070
16. Perrin S. Preclinical research: Make mouse studies work. *Nature*. 2014; 507: 423–5. <https://doi.org/10.1038/507423a> PMID: 24678540
17. Ponsford MJ, Medana IM, Prapansilp P, Hien TT, Lee SJ, Dondorp AM, et al. Sequestration and microvascular congestion are associated with coma in human cerebral malaria. *J Infect Dis*. 2012; 205: 663–671. <https://doi.org/10.1093/infdis/jir812> PMID: 22207648
18. Silamut K, Phu NH, Whitty C, Turner GD, Louwrier K, Mai NT, et al. A quantitative analysis of the microvascular sequestration of malaria parasites in the human brain. *Am J Pathol*. 1999; 155: 395–410. [https://doi.org/10.1016/S0002-9440\(10\)65136-X](https://doi.org/10.1016/S0002-9440(10)65136-X) PMID: 10433933
19. Cêtre C, Pierrot C, Cocude C, Lafitte S, Capron A, Capron M, et al. Profiles of Th1 and Th2 cytokines after primary and secondary infection by *Schistosoma mansoni* in the semipermissive rat host. *Infect Immun*. 1999; 67: 2713–2719. PMID: 10338473
20. Kamiyama T, Cortés GT, Rubio Z. The role of thymocytes and IgG antibody in protection against malaria in nude rats. *Zentralbl Bakteriol Mikrobiol Hyg A*. 1987; 264: 496–501. PMID: 3310466
21. Mercado TI. Paralysis associated with *Plasmodium berghei* malaria in the rat. *J Infect Dis*. 1965; 115: 465–472. PMID: 5845290
22. Smith NC, Favila-Castillo L, Monroy-Ostria A, Hirunpetcharat C, Good MF. The spleen, IgG antibody subsets and immunity to *Plasmodium berghei* in rats. *Immunol Cell Biol*. 1997; 75: 318–323. <https://doi.org/10.1038/icb.1997.48> PMID: 9243299
23. Zuo S, Ge H, Li Q, Zhang X, Hu R, Hu S, et al. Artesunate protected blood-brain barrier via sphingosine 1 phosphate receptor 1/phosphatidylinositol 3 kinase pathway after subarachnoid hemorrhage in rats. *Mol Neurobiol*. 2016; <https://doi.org/10.1007/s12035-016-9732-6> PMID: 26820677
24. Vreden SG, Van den Broek MF, Oettinger MC, Boers W, Van-Rooijen N, Meuwissen JH, et al. Susceptibility to *Plasmodium berghei* infection in rats is modulated by the acute phase response. *Parasite Immunol*. 1995; 17: 445–450. PMID: 8552412
25. Hagendorff A, Dettmers C, Danos P, Hümmelgen M, Vahlhaus C, Martin C, et al. Cerebral vasoconstriction during sustained ventricular tachycardia induces an ischemic stress response of brain tissue in rats. *J Mol Cell Cardiol*. 1998; 30: 2081–94. <https://doi.org/10.1006/jmcc.1998.0772> PMID: 9826520
26. Pearce PS, Friedman D, LaFrancois JJ, Iyengar SS, Fenton AA, MacLusky NJ, et al. Spike-wave discharges in adult Sprague-Dawley rats and their implications for animal models of temporal lobe epilepsy. *Epilepsy Behav*. 2014; 32: 121–131. <https://doi.org/10.1016/j.yebeh.2014.01.004> PMID: 24534480
27. Mengya X, Qingna S, Yiyi W, Yan C, Nan Z. Hydroxysafflor yellow A increases BDNF and NMDARs in the hippocampus in A vascular dementia rat model. *Brain Res*. 2016; <https://doi.org/10.1016/j.brainres.2016.04.030> PMID: 27086971
28. Brown IN, Phillips RS. Immunity to *Plasmodium berghei* in rats: passive serum transfer and role of the spleen. *Infect Immun*. 1974; 10: 1213–8. PMID: 4611920
29. Pierrot C, Adam E, Lafitte S, Godin C, Dive D, Capron M, et al. Age-related susceptibility and resistance to *Plasmodium berghei* in mice and rats. *Exp Parasitol*. 2003; 104: 81–85. [https://doi.org/10.1016/S0014-4894\(03\)00134-6](https://doi.org/10.1016/S0014-4894(03)00134-6) PMID: 12932766
30. Carvalho LJ, Lenzi HL, Pelajo-Machado M, Oliveira DN, Daniel-Ribeiro CT, Ferreira-da-Cruz MF. *Plasmodium berghei*: cerebral malaria in CBA mice is not clearly related to plasma TNF levels or intensity of

- histopathological changes. *Exp Parasitol*. 2000; 95: 1–7. <https://doi.org/10.1006/expr.2000.4508> PMID: 10864512
31. Hearn J, Rayment N, Landon DN, David R, Souza JB De, Katz DR, et al. Immunopathology of Cerebral Malaria: Morphological evidence of parasite sequestration in murine brain microvasculature immunopathology of cerebral malaria: morphological evidence of parasite sequestration in murine brain microvasculature. *Infect Immun*. 2000; 68: 5364–5376. <https://doi.org/10.1128/IAI.68.9.5364-5376.2000> Updated PMID: 10948166
 32. Maitland K, Marsh K. Pathophysiology of severe malaria in children. *Acta Trop*. 2004; 90: 131–140. <https://doi.org/10.1016/j.actatropica.2003.11.010> PMID: 15177139
 33. Boivin MJ, Bangirana P, Byarugaba J, Opoka R, Idro R, Jurek AM, et al. Cognitive impairment after cerebral malaria in children: a prospective study. *Pediatrics*. 2007; 119: 1–14. <https://doi.org/10.1542/peds.2006-1874> Cognitive
 34. Brewster DR, Kwiatkowski D, White NJ. Neurological sequelae of cerebral malaria in children. *Lancet*. 1990; 336: 1039–1043. [https://doi.org/10.1016/0140-6736\(90\)92498-7](https://doi.org/10.1016/0140-6736(90)92498-7) PMID: 1977027
 35. Marsh K, English M, Crawley J, Peshu N. The pathogenesis of severe malaria in African children. *Ann Trop Med Parasitol*. 1996; 90: 395–402.
 36. Idro R, Kakooza-Mwesige A, Balyejussa S, Mirembe G, Mugasha C, Tugumisirize J, et al. Severe neurological sequelae and behaviour problems after cerebral malaria in Ugandan children. *BMC Res Notes*. 2010; 3: 104. <https://doi.org/10.1186/1756-0500-3-104> PMID: 20398391
 37. Molyneux ME, Taylor TE, Wirima JJ, Borgstein A. Clinical features and prognostic indicators in paediatric cerebral malaria: a study of 131 comatose Malawian children. *Q J Med*. 1989; 71: 441–459. PMID: 2690177
 38. Kalinga A, Mayige M, Kagaruki G, Shao A, Mwakyusa B, Jacob F, et al. Clinical manifestations and outcomes of severe malaria among children admitted to Rungwe and Kyela district hospitals in south-western Tanzania. *Tanzan J Health Res*. 2012; 14: 1–9. <https://doi.org/10.4314/thrb.v14i1.2>
 39. Schumacher R-F, Spinelli E. Malaria in children. *Mediterr J Hematol Infect Dis*. 2012; 4: e2012073. <https://doi.org/10.4084/MJHID.2012.073> PMID: 23205261
 40. WHO. Severe malaria. John Wiley & Sons, editor. *Tropical medicine & international health*. 2014. 10.1111/tmi.12313_2
 41. Giha HA, A-Elbasit IE, A-Elgadir TME, Adam I, Berzins K, ElGhazali G, et al. Cerebral malaria is frequently associated with latent parasitemia among the semi-immune population of eastern Sudan. *Microbes Infect*. 2005; 7: 1196–1203. <https://doi.org/10.1016/j.micinf.2005.04.004> PMID: 15994107
 42. Müller Olaf, Traoré Corneille, Albrecht Jahn HB. Severe anaemia in west African children: malaria or malnutrition? 2003; 361: 86–87.
 43. Kateera F, Ingabire CM, Hakizimana E, Kalinda P, Mens PF, Grobusch MP, et al. Malaria, anaemia and under-nutrition: three frequently co-existing conditions among preschool children in rural Rwanda. *Malar J*. 2015; 14: 440. <https://doi.org/10.1186/s12936-015-0973-z> PMID: 26542672
 44. Cserti-Gazdewich CM, Dhabangi A, Musoke C, Ssewanyana I, Ddunga H, Nakiboneka-Ssenabulya D, et al. Inter-relationships of cardinal features and outcomes of symptomatic pediatric *Plasmodium falciparum* malaria in 1,933 children in Kampala, Uganda. *Am J Trop Med Hyg*. 2013; 88: 747–56. <https://doi.org/10.4269/ajtmh.12-0668> PMID: 23358640
 45. Douglas NM, Anstey NM, Buffet PA, Poespoprodjo JR, Yeo TW, White NJ, et al. The anaemia of *Plasmodium vivax* malaria. *Malar J*. 2012; 11: 135. <https://doi.org/10.1186/1475-2875-11-135> PMID: 22540175
 46. Maina RN, Walsh D, Gaddy C, Hongo G, Waitumbi J, Otieno L, et al. Impact of *Plasmodium falciparum* infection on haematological parameters in children living in Western Kenya. *Malar J*. 2010; 9 Suppl 3: S4. <https://doi.org/10.1186/1475-2875-9-S3-S4> PMID: 21144084
 47. Combes V, Coltel N, Faille D, Wassmer SC, Grau GE. Cerebral malaria: role of microparticles and platelets in alterations of the blood-brain barrier. *Int J Parasitol*. 2006; 36: 541–546. <https://doi.org/10.1016/j.ijpara.2006.02.005> PMID: 16600245
 48. Hunt NH, Grau GE. Cytokines: Accelerators and brakes in the pathogenesis of cerebral malaria. *Trends Immunol*. 2003; 24: 491–499. [https://doi.org/10.1016/S1471-4906\(03\)00229-1](https://doi.org/10.1016/S1471-4906(03)00229-1) PMID: 12967673
 49. Rogier C, Gerardin P, Imbert P. Thrombocytopenia is predictive of lethality in severe childhood *falciparum* malaria. *Arch Dis Child*. 2004; 89: 795–6. <https://doi.org/10.1136/adc.2003.045179> PMID: 15269089
 50. Ladhani S, Lowe B, Cole AO, Kowuondo K, Newton CRJC. Changes in white blood cells and platelets in children with *falciparum* malaria: relationship to disease outcome. *Br J Haematol*. 2002; 119: 839–847. <https://doi.org/10.1046/j.1365-2141.2002.03904.x> PMID: 12437669

51. Oluwayemi OI, Brown BJ, Oyedeji OA, Adegoke SA, Adebami OJ, Oyedeji GA. Clinical and laboratory predictors of outcome in cerebral malaria in suburban Nigeria. *J Infect Dev Ctries*. 2013; 7: 600–7. <https://doi.org/10.3855/jidc.2769> PMID: 23949295
52. Kunuanunua TS, Nsibu CN, Gini-Ehangu J-L, Bodi JM, Ekulu PM, Situakibanza H, et al. Acute renal failure and severe malaria in Congolese children living in Kinshasa, Democratic Republic of Congo. *Néphrologie & thérapeutique*. 2013; 9: 160–5. <https://doi.org/10.1016/j.nephro.2013.01.001> PMID: 23402997
53. Centor RM. Serum Total Carbon Dioxide. 1990; 888–889. <http://europepmc.org/abstract/MED/21250150>
54. Dondorp AM, Lee SJ, Faiz M a, Mishra S, Price R, Tjitra E, et al. The relationship between age and the manifestations of and mortality associated with severe malaria. *Clin Infect Dis*. 2008; 47: 151–7. <https://doi.org/10.1086/589287> PMID: 18533842
55. White NJ, Marsh K, Turner RC, Miller KD, Berry CD, Williamson DH, et al. Hypoglycaemia in african children with severe malaria. *Lancet*. 1987; 329: 708–711. [https://doi.org/10.1016/S0140-6736\(87\)90354-0](https://doi.org/10.1016/S0140-6736(87)90354-0)
56. White NJ, Warrell DA, Chanthavanich P, Looareesuwan S, Warrell MJ, Krishna S, et al. Severe hypoglycemia and hyperinsulinemia in falciparum malaria. *N Engl J Med*. 1983; 309: 61–6. <https://doi.org/10.1056/NEJM198307143090201> PMID: 6343877
57. Kawo NG, Msengi AE, Swai AB, Chuwa LM, Alberti KG, McLarty DG. Specificity of hypoglycaemia for cerebral malaria in children. *Lancet*. 1990; 336: 454–7. PMID: 1974988
58. Petithory JC, Lebeau G, Galeazzi G, Chauty A. Hypocalcemia in malaria. Study of correlations with other parameters. *Bull Société Pathol Exot*. 1983; 76: 455–62.
59. Vannaphan S, Walters N, Saengnedsawang T, Tangpukdee N, Kham-in P, Klubprasit M, et al. Factors associated with acute renal failure in severe malaria patients. *Southeast Asian J Trop Med Public Heal*. 2010; 41: 1042–1047.
60. Maitland K, Pamba A, Fegan G, Njuguna P, Nadel S, Newton CRJC, et al. Perturbations in electrolyte levels in kenyan children with severe malaria complicated by acidosis. *Clin Infect Dis*. 2005; 40: 9–16. <https://doi.org/10.1086/426022> PMID: 15614686
61. Nacher M, Treeprasertsuk S, Singhasivanon P, Silachamroon U, Vannaphan S, Gay F, et al. Association of hepatomegaly and jaundice with acute renal failure but not with cerebral malaria in severe falciparum malaria in Thailand. *Am J Trop Med Hyg*. 2001; 65: 828–33. PMID: 11791981
62. Naqvi R, Ahmad E, Akhtar F, Naqvi A, Rizbi A. Outcome in severe acute renal failure associated with malaria. *Nephrol Dial Transplant*. 2003; 18: 1820–1823. <https://doi.org/10.1093/ndt/gfg260> PMID: 12937230
63. May J, Lell B, Luty a J, Meyer CG, Kreamsner PG. Plasma interleukin-10: Tumor necrosis factor (TNF)-alpha ratio is associated with TNF promoter variants and predicts malarial complications. *J Infect Dis*. 2000; 182: 1570–1573. <https://doi.org/10.1086/315857> PMID: 11023485
64. Burgmann H, Hollenstein U, Wenisch C, Thalhammer F, Looareesuwan S, Graninger W. Serum concentrations of MIP-1 alpha and interleukin-8 in patients suffering from acute *Plasmodium falciparum* malaria. *Clinical Immunology and Immunopathology*. 1995. pp. 32–6. <https://doi.org/10.1006/clin.1995.1084> PMID: 7606866
65. de Kossodo S, Grau GE. Profiles of cytokine production in relation with susceptibility to cerebral malaria. *J Immunol*. 1993; 151: 4811–4820. PMID: 8409439
66. Medana IM, Hunt NH, Chaudhri G. Tumor necrosis factor-alpha expression in the brain during fatal murine cerebral malaria: evidence for production by microglia and astrocytes. *Am J Pathol*. 1997; 150: 1473–86. PMID: 9095002
67. John CC, Panoskaltis-Mortari A, Opoka RO, Park GS, Orchard PJ, Jurek AM, et al. Cerebrospinal fluid cytokine levels and cognitive impairment in cerebral malaria. *Am J Trop Med Hyg*. 2008; 78: 198–205. PMID: 18256412
68. Mahanta A, Kar SK, Kakati S, Baruah S. Heightened inflammation in severe malaria is associated with decreased IL-10 expression levels and neutrophils. *Innate Immunity*. 2015. pp. 546–552. <https://doi.org/10.1177/1753425914561277> PMID: 25466232
69. Wenisch C., Parschalk B., Narzt E., E., Looareesuwan S. Elevated Serum Levels of IL-10 and INFg Patients with acute *Plasmodium* Malaria. *Clin Immunol Immunopathol*. 1995; 115–117.
70. Peyron F, Burdin N, Ringwald P, Vuillez JP, Rousset F, Banchereau J. High levels of circulating IL-10 in human malaria. *Clin Exp Immunol*. 1994; 95: 300–3. PMID: 8306505
71. Couper K, Blount D, Riley E. IL-10: the master regulator of immunity to infection. *J Immunol*. 2008; 180: 5771–5777. <https://doi.org/10.4049/jimmunol.180.9.5771> PMID: 18424693

72. Kossodo S, Monso C, Juillard P, Velu T, Goldman M, Grau GE. Interleukin-10 modulates susceptibility in experimental cerebral malaria. *Immunology*. 1997; 91: 536–540. <https://doi.org/10.1046/j.1365-2567.1997.00290.x> PMID: 9378491
73. Li C, Sanni LA, Omer F, Riley E, Langhorne J. Pathology of *Plasmodium chabaudi chabaudi* Infection and Mortality in Interleukin-10-Deficient Mice are ameliorated by anti-tumor necrosis factor alpha and exacerbated by anti-transforming growth factor antibodies. *Infect Immun*. 2003; 71: 4850–4856. <https://doi.org/10.1128/IAI.71.9.4850-4856.2003> PMID: 12933825
74. Wilson KD, Stutz SJ, Ochoa LF, Valbuena GA, Cravens PD, Dineley KT, et al. Behavioural and neurological symptoms accompanied by cellular neuroinflammation in IL-10-deficient mice infected with *Plasmodium chabaudi*. *Malar J.*; 2016; 15: 428. <https://doi.org/10.1186/s12936-016-1477-1> PMID: 27557867
75. Penet MF, Viola A, Confort-Gouny S, Le Fur Y, Duhamel G, Kober F, et al. Imaging experimental cerebral malaria in vivo: significant role of ischemic brain edema. *J Neurosci*. 2005; 25: 7352–7358. <https://doi.org/10.1523/JNEUROSCI.1002-05.2005> PMID: 16093385
76. Rénia L, Potter SM, Mauduit M, Rosa DS, Kayibanda M, Deschemin JC, et al. Pathogenic T cells in cerebral malaria. *Int J Parasitol*. 2006; 36: 547–554. <https://doi.org/10.1016/j.ijpara.2006.02.007> PMID: 16600241
77. Van Der Heyde HC, Bauer P, Sun G, Chang WL, Yin L, Fuseler J, et al. Assessing vascular permeability during experimental cerebral malaria by a radiolabeled monoclonal antibody technique. *Infect Immun*. 2001; 69: 3460–3465. <https://doi.org/10.1128/IAI.69.5.3460-3465.2001> PMID: 11292776
78. Medana IM, Day NP, Sachanonta N, Mai NT, Dondorp AM, Pongponratn E, et al. Coma in fatal adult human malaria is not caused by cerebral oedema. *Malar J*. 2011; 10: 267. <https://doi.org/10.1186/1475-2875-10-267> PMID: 21923924
79. Mohanty S, Mishra SK, Patnaik R, Dutt AK, Pradhan S, Das B, et al. Brain swelling and mannitol therapy in adult cerebral malaria: a randomized trial. *Clin Infect Dis*. 2011; 53: 349–55. <https://doi.org/10.1093/cid/cir405> PMID: 21810747
80. Medana IM, Turner GDH. Human cerebral malaria and the blood-brain barrier. *Int J Parasitol*. 2006; 36: 555–68. <https://doi.org/10.1016/j.ijpara.2006.02.004> PMID: 16616145
81. Newton CR, Crawley J, Sowumni A, Waruiru C, Mwangi I, English M, et al. Intracranial hypertension in Africans with cerebral malaria. *Arch Dis Child*. 1997; 76: 219–26. <https://doi.org/10.1136/adc.76.3.219> PMID: 9135262
82. Newton CRJC, Marsh K, Peshu N, Kirkham FJ. Perturbations of cerebral hemodynamics in Kenyans with cerebral malaria. *Pediatr Neurol*. 1996; 15: 41–49. [https://doi.org/10.1016/0887-8994\(96\)00115-4](https://doi.org/10.1016/0887-8994(96)00115-4) PMID: 8858700
83. Milner DA, Whitten RO, Kamiza S, Carr R, Liomba G, Dzamalala C, et al. The systemic pathology of cerebral malaria in African children. *Front Cell Infect Microbiol*. *Frontiers*; 2014; 4: 104. <https://doi.org/10.3389/fcimb.2014.00104> PMID: 25191643
84. Seydel KB, Kampondeni SD, Valim C, Potchen MJ, Milner DA, Muwalo FW, et al. Brain swelling and death in children with cerebral malaria. *N Engl J Med*. 2015; 372: 1126–37. <https://doi.org/10.1056/NEJMoa1400116> PMID: 25785970
85. Newton CR, Peshu N, Kendall B, Kirkham FJ, Sowumni A, Waruiru C, et al. Brain swelling and ischaemia in Kenyans with cerebral malaria. *Arch Dis Child*. 1994; 70: 281–7. PMID: 8185359
86. Dorovini-Zis K, Schmidt K, Huynh H, Fu W, Whitten RO, Milner D, et al. The neuropathology of fatal cerebral malaria in malawian children. *Am J Pathol*. 2011; 178: 2146–58. <https://doi.org/10.1016/j.ajpath.2011.01.016> PMID: 21514429
87. Taylor TE. Caring for children with cerebral malaria: insights gleaned from 20 years on a research ward in Malawi. *Trans R Soc Trop Med Hyg*. 2009; 103: 6–10. <https://doi.org/10.1016/j.trstmh.2008.10.049> PMID: 19128813
88. Oo MM, Aikawa M, Than T, Aye TM, Myint PT, Igarashi I, et al. Human Cerebral Malaria. *J Neuropathol Exp Neurol*. 1987; 46: 223–231. <https://doi.org/10.1097/00005072-198703000-00009> PMID: 3546601
89. White VA, Lewallen S, Beare N, Kayira K, Carr RA, Taylor TE. Correlation of retinal haemorrhages with brain haemorrhages in children dying of cerebral malaria in Malawi. *Trans R Soc Trop Med Hyg*. 2001; 95: 618–621. [https://doi.org/10.1016/S0035-9203\(01\)90097-5](https://doi.org/10.1016/S0035-9203(01)90097-5) PMID: 11816433
90. Taylor-Robinson AW. Validity of modelling cerebral malaria in mice: argument and counter argument. *J Neuroparasitology*. 2010; 1: 45–49. <https://doi.org/10.4303/jnp/N100601>
91. Baptista FG, Pamplona A, Pena AC, Mota MM, Pied S, Vigário AM. Accumulation of *Plasmodium berghei*-infected red blood cells in the brain is crucial for the development of cerebral malaria in mice. *Infect Immun*. 2010; 78: 4033–4039. <https://doi.org/10.1128/IAI.00079-10> PMID: 20605973

92. Dende C, Meena J, Nagarajan P, Panda AK, Rangarajan PN, Padmanaban G. Simultaneously targeting inflammatory response and parasite sequestration in brain to treat Experimental Cerebral Malaria. *Sci Rep*. 2015; 5: 12671. <https://doi.org/10.1038/srep12671> PMID: 26227888
93. Piva L, Tetlak P, Claser C, Karjalainen K, Renia L, Ruedl C. Cutting edge: Clec9A+ dendritic cells mediate the development of experimental cerebral malaria. *J Immunol*. 2012; 189: 1128–32. <https://doi.org/10.4049/jimmunol.1201171> PMID: 22732587
94. Schmittgen TD, Livak KJ. Analyzing real-time PCR data by the comparative CT method. *Nat Protoc*. 2008; 3: 1101–1108. <https://doi.org/10.1038/nprot.2008.73> PMID: 18546601
95. Uyama O, Okamura N, Yanase M, Narita M, Kawabata K, Sugita M. Quantitative evaluation of vascular permeability in the gerbil brain after transient ischemia using Evans blue fluorescence. *J Cereb Blood Flow Metab*. 1988; 8: 282–284. <https://doi.org/10.1038/jcbfm.1988.59> PMID: 3343300
96. Bopp SE, Rodrigo E, González-Páez GE, Frazer M, Barnes S, Valim C, et al. Identification of the *Plasmodium berghei* resistance locus 9 linked to survival on chromosome 9. *Malar J*. 2013; 12: 316. <https://doi.org/10.1186/1475-2875-12-316> PMID: 24025732